

**FACULTY
OF MECHANICAL
ENGINEERING
CTU IN PRAGUE**

Development of a method to predict bolt loosening

Thibault DUGAST

03/04/2023 – 15/09/2023

Study programme: Master of Automotive Engineering

Specialization: Advanced powertrains

CTU supervisor: Lukáš Pacoň



MASTER'S THESIS ASSIGNMENT

I. Personal and study details

Student's name: **Dugast Thibault** Personal ID number: **515082**
 Faculty / Institute: **Faculty of Mechanical Engineering**
 Department / Institute: **Department of Automotive, Combustion Engine and Railway Engineering**
 Study program: **Master of Automotive Engineering**
 Branch of study: **Advanced Powertrains**

II. Master's thesis details

Master's thesis title in English:

Development of a Method to Predict Bolt Loosening

Master's thesis title in Czech:

Vývoj metody předvídání povolování šroubů

Guidelines:

Objectives:

- To investigate the factors that contribute to bolt loosening in complex assemblies
- To develop a method that accurately predicts the likelihood of bolt loosening in complex assemblies
- To validate the effectiveness of the method through a simulation

Methodology:

- Review existing literature on bolt loosening and related phenomena
- Conduct analytical research using Thomala's method to develop a general formula for predicting bolt loosening
- Optimize the model to gather necessary information and modify the formula to apply to complex assemblies
- Validate the method through simulations and experiments

Expected Results:

- A method for predicting the likelihood of bolt loosening in complex assemblies
- A better understanding of the factors that contribute to bolt loosening in complex assemblies

Deliverables:

- A final thesis summarizing the research, methodology, results, and conclusions


Name and workplace of master's thesis supervisor:

Ing. Lukáš Pacoň

Name and workplace of second master's thesis supervisor or consultant:

Date of master's thesis assignment: **30.04.2023** Deadline for master's thesis submission: **11.08.2023**

Assignment valid until: _____


 Ing. Lukáš Pacoň
 Supervisor's signature



 doc. Ing. Oldřich Vitek, Ph.D.
 Head of department's signature


 doc. Ing. Miroslav Španiel, CSc.
 Dean's signature

III. Assignment receipt

The student acknowledges that the master's thesis is an individual work. The student must produce his thesis without the assistance of others, with the exception of provided consultations. Within the master's thesis, the author must state the names of consultants and include a list of references.

21/06/2023
 Date of assignment receipt


 Student's signature

Acknowledgements

I am very grateful to Guillaume HELLER and Massimo BRUNO who ran the recruiting process along with my technical tutor Olivier MASSAROTTO. They entrusted me this 5-month Research & Development project and even accepted it to be published to the public despite being confidential, since it was necessary for my internship for the Czech Technical University.

I would like to recognize the numerical simulation team who worked with me. They shared their work with me and introduced me to the industrial numerical simulation world.

I also want to acknowledge my tutor at Czech Technical University Lukáš Pacoň who followed my work for 5 months, and Gabriela Achtenová and Monika Matyášová for following me with the administrative paperwork.

Finally, I would like to express my deepest appreciation to my tutor Olivier MASSAROTTO for always giving me the help I needed while entrusting me the management of this project. I was able to learn a lot from him and improve in many technical areas tackled by this internship.

Abstract

This thesis report of my 5-month internship explains the different possibilities I explored in order to reduce the loosening of the screws of a wheel by optimizing its design. Indeed, spontaneous loosening is a major issue in most bolted assemblies undergoing vibratory forces. These cyclic loadings can sometimes lead to spontaneous loosening of the bolts or screws, especially if the assembly was not correctly dimensioned. Despite all that, a lot of research has been done about screws loosening, but very few tackled the solving of this issue especially because many of these cases can be answered by using an additional system, which were not what we wanted. Therefore, to prevent this, the main points studied were the understanding and measuring of loosening in a general assembly, and the change of different design aspects to reduce the loosening previously measured.

To understand and measure loosening, I compared a simple bolted assembly with that of Cobra software, which is able to predict loosening for small and simple assemblies. I also compared the results with Thomala's method, a technique comparing the displacement of the screw with that of a theoretical beam. I also had to get a wheel model to optimize with OptiStruct, which I got by converting a previous Abaqus model given by Segula. Finally, I used my formerly acquired knowledge to change its design and improve the non-loosening of the four screws.

To conclude, I modelled an optimized version of the wheel with a decreased loosening of the screws, and compared these results with the initial version. I also conclude on the influence of the various parameters on loosening, in the specific case of the wheel, which could somewhat be extrapolated to other bolted assemblies.

Keywords

Spontaneous loosening – Bolted assembly – Finite Elements Analysis – Thomala - Optimization

Declaration of authorship

I hereby declare that I am the sole author of the thesis titled “Development of a method to predict bolt loosening”.

I duly marked out all quotations. The used literature and sources are stated in the list of references.

In Brognard: 11/08/2023

Thibault Dugast

For confidentiality reasons, some values (mostly sections 4 and 5) in this report were hidden, and others were changed not to match those of the confidential parts given by Segula.

However the general reasoning is kept the same, and the conclusions drawn match those which were obtained with the correct values.

Table of content

Abstract	4
Keywords	4
List of figures	8
Glossary	9
1. R&D activities for Segula company	11
1.1. Scientific approach	12
1.2. Objectives and issues.....	12
2. Literature review	13
2.1. Current different designs.....	13
2.2. Aim of the study	13
2.3. Loosening definition and characterisation	15
2.3.1. Loosening definition.....	15
2.3.2. Interests and practical examples.....	17
2.3.3. Standardised tests	17
2.4. Previous analytical and numerical studies on loosening.....	19
2.4.1. Analytical studies of the various models.....	19
2.4.2. Numerical studies of the various models.....	23
2.5. Previous experimental studies on loosening.....	27
2.5.1. Experimental studies using 1 screw	28
2.5.2. Experimental study using 2 screws	28
2.6. Influence of assembly design on loosening.....	29
2.6.1. Shape of the assembly	30
2.6.2. Assembly parallilism	30
2.6.3. Assembly flatness	30
2.7. Previous work	32
2.8. Literature review critique	33
3. Numerical loosening study	34
3.1. Cobra V6 loosening comparisons	34
3.2. Thomala’s method	38
4. Wheel model conversion	41
4.1. Automatic conversion.....	41
4.2. Material properties conversion	41

4.3.	Membranes conversion	41
4.4.	Contacts conversion	42
4.4.1.	Contact definition.....	42
4.4.2.	Contact properties	46
4.5.	Model steps conversion.....	46
4.6.	Non-linear static parameters.....	47
4.7.	Mesh optimization for reduced computing time	47
4.8.	Models comparison	48
4.8.1.	Displacements comparison	48
4.8.2.	Slips comparison.....	49
4.8.3.	Pressures comparison	51
4.8.4.	Screw angles and loosening	53
4.9.	Conversion conclusion.....	55
5.	Wheel design optimization.....	56
5.1.	Manual optimization	56
5.1.1.	Linear and quadratic regressions	56
5.1.2.	Optimization with parameters variations	58
5.1.3.	Shape changes.....	61
5.2.	Automatic optimization.....	63
5.3.	Loosening prediction	63
6.	Conclusion	65
7.	Further possible research and improvements	67
	Sources.....	68

List of figures

Figure 1 : Summary of Segula influence	11
Figure 2 : Segula's clients	11
Figure 3 : Gantt chart	12
Figure 4 : Different rim designs	13
Figure 5 : Static and dynamic friction cones	14
Figure 6 : Different loosening stages	16
Figure 7 : Relation between localised slip and complete slip	16
Figure 8 : Junker ISO 16130 test set-up	18
Figure 9 : NAS/NASM test set-up	18
Figure 10 : NF E 25-005 test set-up	19
Figure 11 : Preload uncertainty	21
Figure 12 : Zarwel's model for a screw loosening	24
Figure 13 : Unscrewing of the assembly obtained for the previous configuration	24
Figure 14 : Appearance of under-head slippage during screw bending	25
Figure 15 : Model of 2 plates maintained by a bolt	25
Figure 16 : Axial load in the screw and rotation of the nut in relation to the screw	26
Figure 17 : Loosening of 2 bolts with different stiffness	26
Figure 18 : Influence of bolt spacing	27
Figure 19 : Junker test loosening curves by Zarwel and Ksentini	28
Figure 20 : Bolted assembly with 2 bolts	29
Figure 21 : Bolts loosening with and without shifting the load axis	30
Figure 22 : Stress propagation in the plates	31
Figure 23 : Cross-section of the parts clamped by the screw	31
Figure 24 : Meshed model of the wheel (Abaqus model)	32
Figure 25 : Cobra results for a non-loosening assembly	34
Figure 26 : OptiStruct model of the simple Cobra assembly	35
Figure 27 : Results of the 16 models on the screw (top) and the upper plate (bottom)	36
Figure 28 : Contacts on the simple OptiStruct model	37
Figure 29 : Screw head contact with the upper plate at 501N of external load, slip (green) and stick (red) regions	37
Figure 30 : Geometric parameters for the simple Cobra model in OptiStruct	40
Figure 31 : Node to Surface contact discretization	43
Figure 32 : Surface to Surface contact discretization	43
Figure 33 : Adjust parameter for penetration or separation	44
Figure 34 : Contact pressure on the disk in contact with the hub, with n2s (left) and s2s (right) discretization	45
Figure 35 : Pretension section of a screw in green	46
Figure 36 : Displacements of the wheel with Abaqus (left) and OptiStruct (right)	48
Figure 37 : Slip distances on the rim with the disk, with Abaqus (left) and OptiStruct (right)	50
Figure 38 : Slip distances on the disk with the hub, with Abaqus (left) and OptiStruct (right)	51
Figure 39 : Contact pressures between the disk and the hub, with Abaqus (left) and OptiStruct (right)	52

Figure 40 : Contact pressures between the disk and the rim, with Abaqus (left) and OptiStruct (right).....	52
Figure 41 : <i>ABC</i> angle definition for post processing measurement	53
Figure 42 : Screw angles for the 2 models	54
Figure 43 : Screws numbering on the wheel.....	54
Figure 44 : Screws loads for the 2 models	55
Figure 45 : Warped rim arc on the wheel	59
Figure 46 : Conics cross-section with third point y-coordinate and ratio.....	59
Figure 47 : Parameters used for the manual optimization	60
Figure 48 : Coefficients of the linear regression	60
Figure 49 : Inner rim design improvement	61
Figure 50 : Measurement of the angle of the cone on the screw	62
Figure 51 : Cones design improvement.....	62
Figure 52 : Screw parameters to predict loosening of the wheel.....	63

Glossary

(a_1, \dots, a_{n+1})	Coefficients of the regression
C_0	Tightening torque
d	Screw nominal diameter
d_2	Sidewall diameter (inside of the threads)
d_t	Diameter under the screw head
E	Young's modulus (for the screw)
F_{ax}	External axial load on the screw
F_t	External transverse load on the screw
F_0	Screw preload or screw pretension
F_0^+	Upper range of the practical tightening preload
F_0^-	Lower range of the practical tightening preload
$F_{0,max}$	Maximal tightening preload tolerated by the assembly
$F_{0,min}$	Minimal tightening preload for the assembly
ΔF_z	Decrease in preload after tightening (non-rotational component)
G	Shear modulus for the screw
I	Second moment of area (for the screw)

k	Shear correction coefficient for a cylinder
L	Useful screw length between plates
ΔL_c	Elongation due to creep
ΔL_s	Elongation due to strain hardening of the joint surfaces
p	Screw pitch
R^2	Coefficient of determination
S_{eq}	Equivalent resistant cross-section
SS_{res}	Sum of Squares of residuals
(x_1, \dots, x_n)	Parameters used in the regression
y	Screw tension for the regression
\hat{y}	Screw tension approximation by the regression
β	Load introduction coefficient
δ_{crit}	Threshold displacement of the screwhead before it loosens
$\delta_{crit,E.B}$	Threshold displacement of the screwhead for Euler-Bernoulli's theory
$\delta_{crit,T}$	Threshold additional displacement of the the screw head for Timoshenko's theory
δ_p	Plate flexibility
δ_s	Screw flexibility
λ	Filtering coefficient
μ	Global friction coefficient under the head and between the threads
μ_h	Friction coefficient under the head
μ_t	Friction coefficient between the threads
$\mu_{p,min}$	Minimum friction coefficient between the plates

1. R&D activities for Segula company

Segula technologies is a French engineering group present in 30 countries in the world. It is mainly involved in the major industrial sectors like automotive, aerospace & defence, energy, life sciences, naval and rail industries.



Figure 1 : Summary of Segula influence

Segula Technologies owns 5 main agencies in France: Trappes, La Ferté-Vidame, Bron, Rennes and Brognard where my internship takes place. This Specific Brognard site contains chassis engineering, synthesis and numerical simulation, processes and production systems as well as Research and Development as its main activities. Its automotive clients are among the top vehicle manufacturers like Stellantis, Mercedes-Benz, BMW and Audi, as well as equipment manufacturers like Valeo and Plastic Omnium.



Figure 2 : Segula's clients

The Brognard agency is involved in Research and Development, therefore my intership project was made to answer one of these Research aspects, while remaining a project internal to Segula Technologies.

1.1. Scientific approach

My internship being part of a Research & Development activity, there was no initial plan for my 5 months of work, hence the Gantt chart below only considers the work done and not the work planned since these plans could completely change depending on the results and the approach we choose to follow. Therefore, this Gantt chart displays the actual work I did during my first 19 weeks.

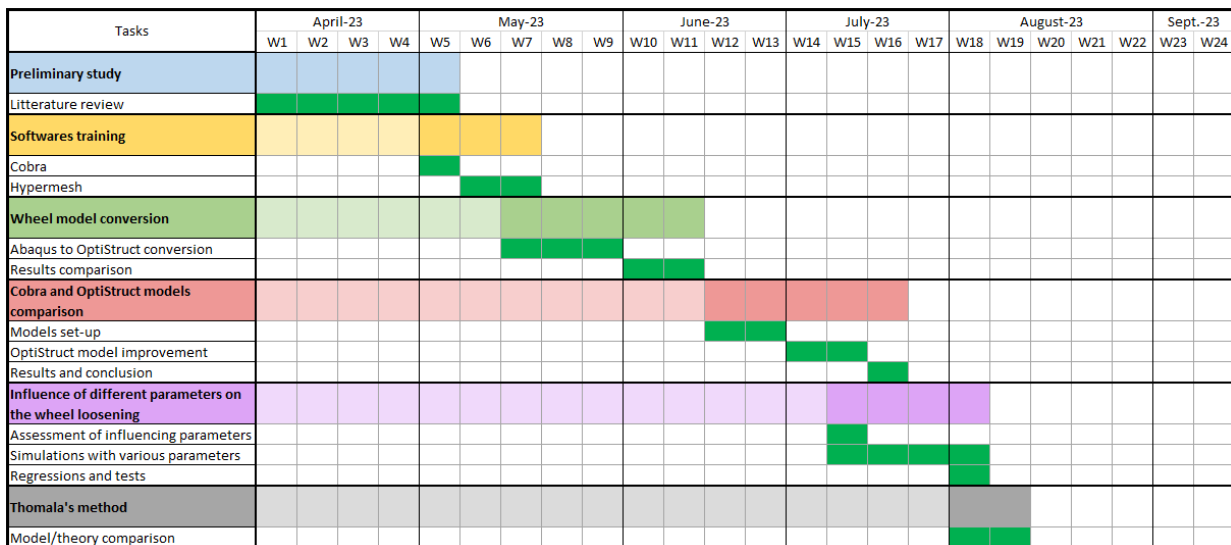


Figure 3 : Gantt chart

1.2. Objectives and issues

This research project focuses on the loosening aspect of the screws of a wheel of a vehicle. Since the efforts regularly applied to a wheel can loosen the screws or bolts which are tightened to the rim, this can lead to these parts detach from the wheel, thus removing the fixations of the different parts of the wheel.

Although some systems exist to reduce this type of loosening, we will try in this study to reduce the loosening of the screws by changing the design of the different components of the current wheel.

This is why this master thesis report called “Development of a method to predict bolt loosening” will also deal with the more general project of my internship called “Optimization of a wheel design to reduce loosening”. Hence the prediction of loosening will play an important role in this optimization project.

2. Literature review

2.1. Current different designs

There are currently a number of different wheel designs, particularly for rims, which can be of several shapes, beyond a circular outer part in the shape of the tyre. The variation then takes place inside the rim, and different structures exist to firmly connect the wheel axle to the tyre.

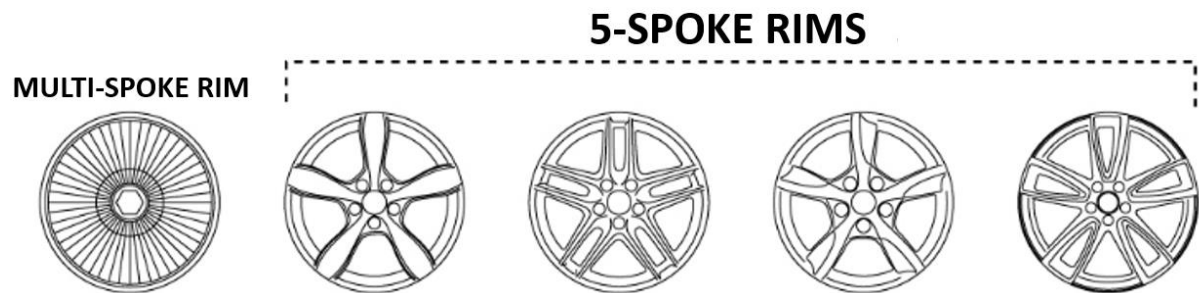


Figure 4 : Different rim designs

These different designs contain radial sections for structural strength. The materials used are generally aluminium or sheet metal. However, of the rims shown in Figure 4, 5-spoke rims are mainly used on classic vehicles, while commercial vehicles prefer multi-spoke rims.

2.2. Aim of the study

This problem of spontaneous loosening is well-known and common, and systems have already been designed to limit it (1).

Some of them, such as notched washers, increase friction under the screw head. However, these are ineffective in terms of vibration, and their use is mainly for flat-screwed assemblies. In our case, there is no real plane under the screw head, and the surface area over which friction could be maximised is very small. Finally, this solution is very ineffective for vibratory loads, as it will be the case for our wheel for most of its service life.

Other systems also increase friction in the threads, such as nylon ring nuts. However, these only slightly reduce loosening under vibratory loads, and cannot be implemented for tapped screws, which would require the screws in the current assembly to be redesigned as well.

There are also locknut systems that limit this loosening. However, vibratory loads are not really affected by this solution, which is also more costly to implement in terms of time and resources.

Rotation-locking solutions such as wire brakes can also be considered, but these do not preserve the preload of the screws and require special screws as well.

Finally, self-locking washers with ramps or safety nuts with ramp washers are expensive to install on all the bolts of the wheels of a vehicle.

These technologies are not sufficient to solve our loosening problem, because none of them satisfies the static, dynamic and vibratory cases while remaining affordable. The approach adopted here is to modify the design of the rim so that this new design reduces the loss of tension in the bolts after loading the wheel.

The parameters that can be studied are the general shape of the rim, its thickness, the friction between the parts, the type of bolt (conical shape of the washer), and any other useful parameter that can be modified.

About the thickness of the rim, the thickness of the part is important for loosening, as will be seen in section 2.4.2.

As far as friction is concerned, increasing friction can be beneficial to prevent loosening: with a higher friction coefficient (shown in Figure 5), and/or a larger friction surface, the normal tightening force applied by the screws will make it easier to maintain the relative position of the parts assembled, and this undergoing higher tangential forces.

Let N be the normal force applied by the screw to the assembly, and f (and f_s) the friction coefficient (static), we obtain T the tangential force applied by the screw head to the rim.

In the static case for a low external tangential force, the screw applies another tangential force T equal in norm and opposite in direction to the external one, so that it cancels this force and prevents any relative movement between these two parts. For an external tangential force greater than $f_s N$, there is relative movement between the parts, and the screw only applies a force $T = f N$ which opposes the movement.

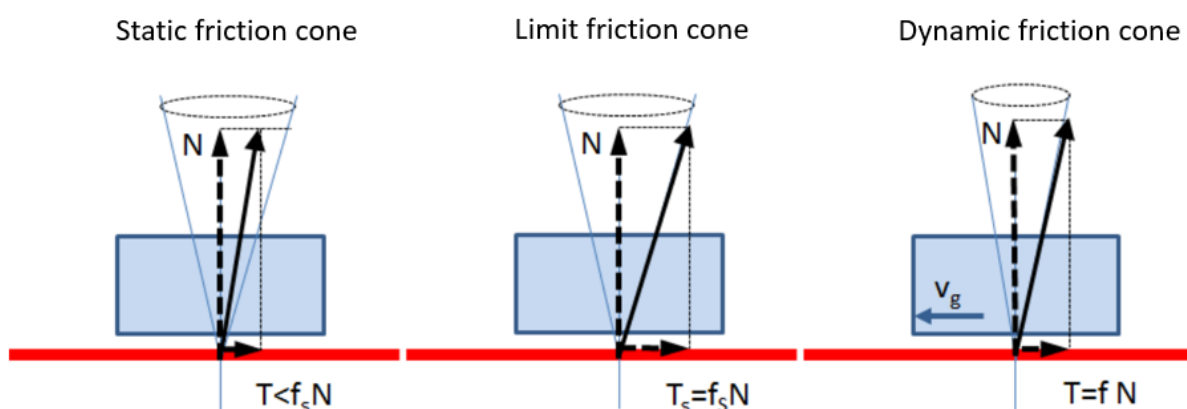


Figure 5 : Static and dynamic friction cones

2.3. Loosening definition and characterisation

2.3.1. Loosening definition

In the case of screwed joints, the physical phenomenon leading to the loss of tension in the screw, following the loading of the parts being joined, is known as spontaneous loosening (1).

Two phenomena can be differentiated by the relative movement between the screw and the nut:

- Loosening only takes into account the loss of tension when the screw and nut's positions are fixed in relation to each other and can be caused by settlement (parts settling into each other), creep (permanent deformation after long-term loading) or matting (plastic deformation caused by high pressure).
- Spontaneous unscrewing then occurs during rotation of the nut relatively with the screw, or simply during rotation of the screw relatively with the thread.

Hence, to characterise the overall loosening of the bolt, which will take into account the previous loosening and the spontaneous unscrewing, it is necessary to study the drop in tension induced in the screw, i.e. the loss of preload in the screw. During the first phase of loosening, matting and strain hardening phenomena reduce this preload without any relative movement nor rotation between the elements, which invalidates the study of loosening based only on the relative rotation between the screw and the nut.

A lot of research has been carried out to characterise the phenomenon of loosening, including analytical, numerical and experimental studies. These studies generally agree on dividing loosening into 4 successive phases (2), as shown in Figure 6:

- Initially, the assembled parts and the screw are all immobile.
- The external forces exceed the forces induced by the screw preload and the assembled parts slide in relation to each other, but the screw head remains fixed with its part. The screw therefore begins to bend and a small amount of slip is introduced into the threads of the screw, known as "localised slip".
- The screw continues to bend until it reaches an extreme position of maximum displacement known as the "critical threshold", at which point the screw head slips on its part. It is during this stage that the loosening mainly occurs.

The screw returns to a position that no longer allows relative movement between the head and the part.

Loosening is not reached when the screw head position does not exceed this threshold critical displacement, or when it does not slip at all.

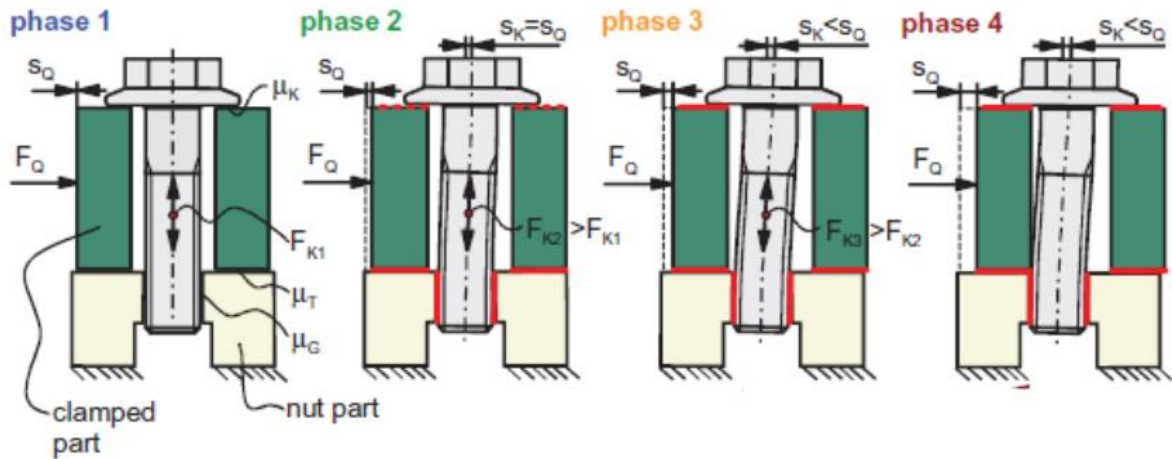


Figure 6 : Different loosening stages

It was also concluded that spontaneous unscrewing was necessarily induced by complete slip of the nut or bolt head, based on the relative movement of the assembled parts. Spontaneous unscrewing therefore cannot occur by relative movement of the assembled parts alone, without slippage of different parts of the bolt.

Hao Gong (1) explains the link between the theories of localised slip and complete slip in Figure 7, which summarises the behaviour of parts concerning slip. Even if the slip is only local initially, the tiny loosening it leads to then can increase the slip, which then propagates into full slip, under the screw head or in the threads, leading to significant loosening.

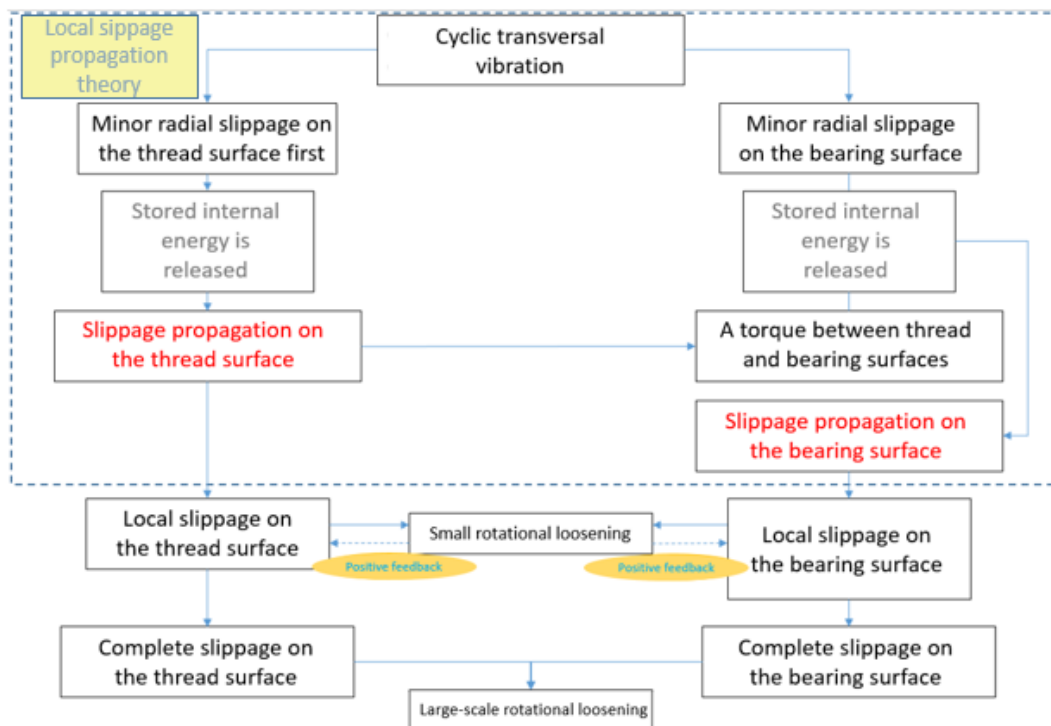


Figure 7 : Relation between localised slip and complete slip

2.3.2. Interests and practical examples

The study of loosening is mainly carried out to avoid loss of pretension in the screws. Reducing the pretension has an impact on the fixing of the assembled parts, which must generally not move. Too much slippage of the assembled parts following the loosening of the bolts can lead to transverse forces between the assembled parts and shear in the bolts in the assembly. However, the numerous parameters taken into account make this a complex study, requiring in-depth numerical, analytical and experimental analyses.

The phenomenon of loosening can occur following different load cases on the assembled parts: transverse loading (perpendicular to the axis of the bolts), axial loading (parallel to the axis of the bolts) centered on the assembly, off-center axial loading, loading rotating around the axis of the assembly, etc. (2), as well as torsional, flexural and impact loading on the assembly (3).

Among these load cases, Aziz (4) showed that axial loading on a correctly sized bolted joint could not lead to spontaneous loosening. It was also shown experimentally that transverse loading was the most likely to cause loosening (at similar loading values). It is therefore the one that will mainly be followed in this literature review, in addition to being the load case for our wheel. The other loadings mentioned above are not studied here, although theoretically possible but neglected.

2.3.3. Standardised tests

Numerous tests have been carried out to try and characterise the loosening according to different assembly configurations, in order to characterise the impacting properties and the value of this loosening.

The ISO 16130 "Junker" test involves stressing the fastener to be tested with an alternating transverse movement. The test device consists of a movable plate assembled to a fixed support, both linked by the fastener to be tested. A rotary motor applies the alternating transverse movement to the mobile support via an eccentric. The following parameters can be set and adjusted:

- The frequency (between 10 and 15 Hz according to ISO 16130 standard)
- The displacement of the tray

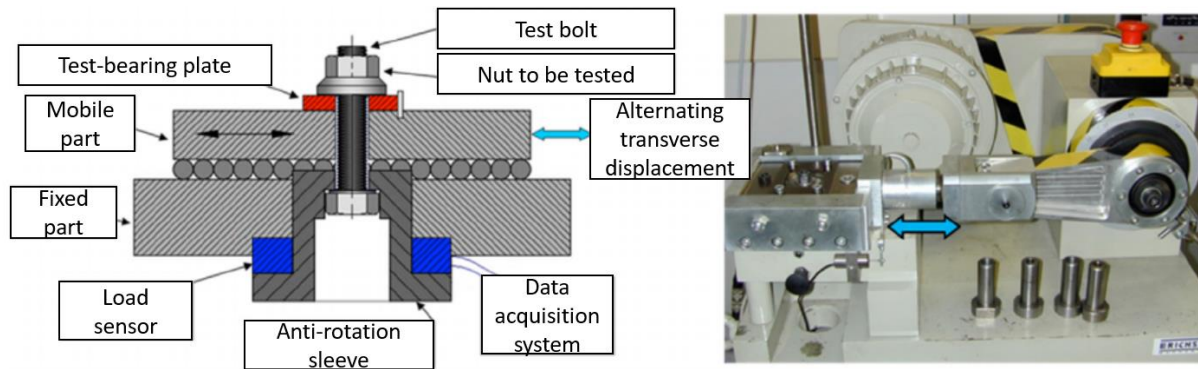


Figure 8 : Junker ISO 16130 test set-up

During this test, the nut tightened on the 2 plates is subjected to vibrations by the relative movement between the fixed plate and the moving plate. It is then possible to measure the loosening of the screw with the reduction in screw force measured by the force sensor.

In order to highlight the loosening of the nut, it is also possible to measure and even observe the position of the bolt after the test. However, this angular position only takes into account the spontaneous loosening and not the first loosening as seen in paragraph 2.3.

Bearings between the two assembled parts also minimise friction between these two parts, although often the loading is not an imposed displacement but a transverse force with friction between the two parts. This test then highlights the loosening of the screws due to the relative rotation between the nut and the head of the screw, created by the stresses.

The NAS 3350, NASM 1312-7 ISO 7481 and ISO 8642 tests use an oblong hole test fixture carried by a vibrating pot. This vibrating pot generates shocks on the fixture at a frequency of around 30 Hz, for a defined displacement, in this case, 11,4 mm.

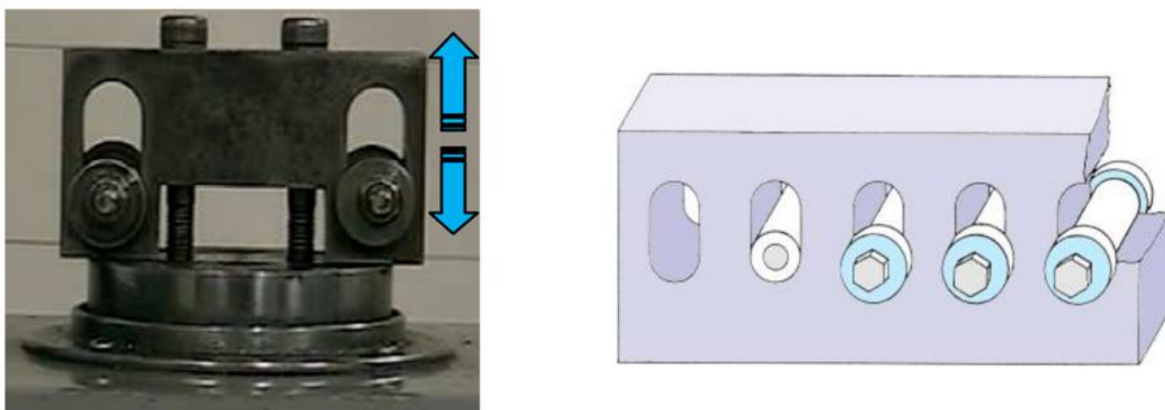


Figure 9 : NAS/NASM test set-up

Finally, the NF E 25-005 test also stresses the fastener by impacts in a similar way to the previous test, at a frequency of approximately 22 Hz, and a displacement of 22,8 mm here.

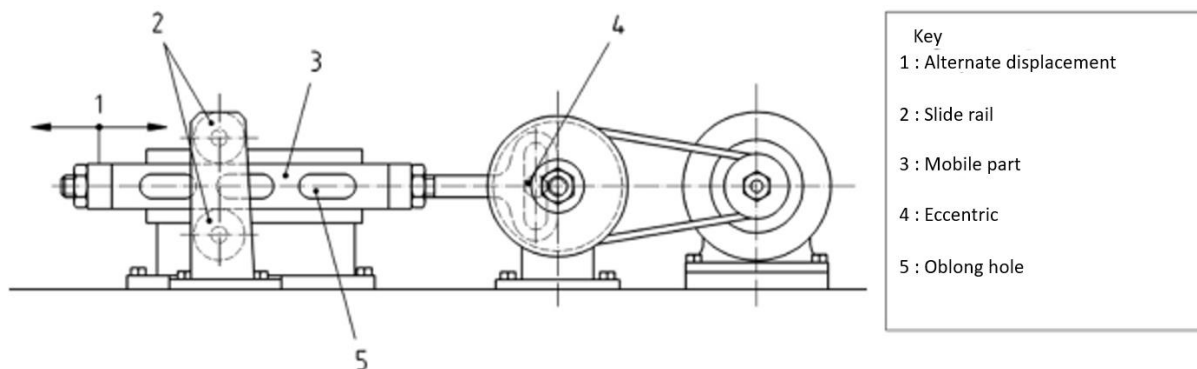


Figure 10 : NF E 25-005 test set-up

There are also other non-standardised tests, such as the Clark and Cook test, the Pearce test and the test by Sase et al. (5). The aim of each of these tests is to demonstrate the loosening of screws under different cyclic loads, without having to measure the loss of tension within the screw if it has loosened sufficiently.

2.4. Previous analytical and numerical studies on loosening

In order to characterise this loosening, several methods were used to determine this criterion analytically, then numerically for greater precision and correlation with reality.

Despite a good amount of research in the field, to date, no model has been able to correctly predict the loosening behaviour of a bolt or screw connection (6). Analytical approaches alone only take part of the problem into account and neglect some of the contact forces by simplifying the problem.

2.4.1. Analytical studies of the various models

Although calculations for screwed assemblies have had many years to be refined, the main difficulty lies in the multitude of contacts between the parts, resulting in numerous and sometimes unknown forces in the system, which make these calculations very complex and the analytical studies arduous.

First of all, it is useful to determine the relationship between the tightening torque and the preload force transmitted to the screw, taking into account the helical screw, the friction in

the threads and the friction under the head. This gives the Kellerman and Klein relationship according to DIN 946 standard:

$$C_0 = F_0 \left(0.16p + 0.58\mu_t d_2 + \frac{\mu_h d_t}{2} \right) \quad (2.1)$$

With:

p the screw pitch

μ_t the friction coefficient between the threads

μ_h the friction coefficient under the head

d_2 the sidewall diameter (inside of the threads)

d_t the diameter under the screw head

Thus, in the event of a loosening, if the only forces to be taken into account are those of the previous relationship, it is possible to determine the minimum friction to be obtained in order to maintain the assembly in position so that loosening does not occur:

$$\mu > \frac{0.16p}{0.58d_2 + \frac{d_t}{2}} \quad (2.2)$$

This result is only true if both friction coefficients are approximated to the same value, i.e. with $\mu_t = \mu_h = \mu$, and in the case where no external force affects the structure. However, in our case, the spontaneous loosening is caused by an external force on the wheel, so this relationship is not sufficient, but developed further.

This relationship from Kellerman and Klein also makes it possible to determine the force F_0 from the torque C_0 , again using the same approximation with the same friction coefficient. This means that tightening the bolt with the torque gives the preload force via a coefficient:

$$F_0 = \frac{C_0}{\left(0.16p + \mu \left(0.58d_2 + \frac{d_t}{2} \right) \right)} \quad (2.3)$$

This relationship therefore allows us to obtain the preload using 2 uncertainties: the uncertainty of the tightening torque between C^- and C^+ with the precision of the tightening method, and the difference made by approximating $\mu_f = \mu_t = \mu$ located between extreme values μ^- et μ^+ .

From these two uncertainties, we obtain a frame of the preload F_0 with $F_0^- = f(C^-, \mu^+)$ and $F_0^+ = f(C^+, \mu^-)$

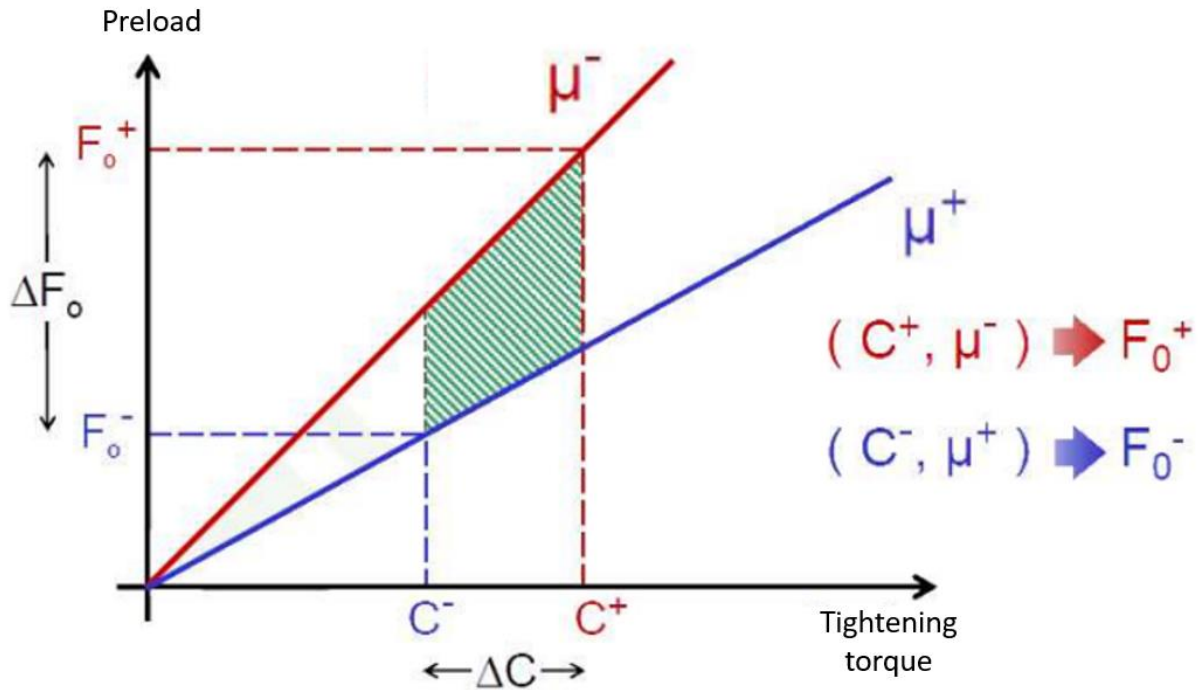


Figure 11 : Preload uncertainty

There is also a torque and angle tightening method in the plastic domain, which allows a lower overall uncertainty on the preload, but with another uncertainty on the angle.

Thus it is necessary to keep this ΔF_0 interval in the range $[F_{0,min}; F_{0,max}]$, which is the range for screw preload for the assembly.

$F_{0,max}$ is generally imposed up to 90% of the elastic limit of the screw, or to guarantee the mechanical strength of all the components of the assembly.

$F_{0,min}$ is chosen to maintain contact between the parts and transmit the forces, after the initial loss of preload due to service and temperature settling, and while taking account of the external forces. We therefore have:

$$F_{0,min} = (1 - \lambda)F_{ax} + \frac{F_t}{\mu_{p,min}} + \Delta F_z \quad (2.4)$$

With:

F_{ax} the external axial load on the screw

F_t external transverse load on the screw

$\mu_{p,min}$ the minimum friction coefficient between the plates

ΔF_z the decrease in preload after tightening

λ the filtering coefficient such that $\lambda = \beta \frac{\delta_s}{\delta_s + \delta_p}$

β the load introduction coefficient

δ_s and δ_p the flexibilities for the screw and the plates

This decrease in preload ΔF_z adds up the settling of joint surfaces ΔF_{L_s} , the decrease in preload due to creep ΔF_{L_c} and the decrease due to temperature changes, which we will not study. Their expressions are as follows:

$$\Delta F_{L_s} = \frac{\Delta L_s}{\delta_s + \delta_p} \quad (2.5)$$

With $\Delta L_s = 0.00329 * \left(\frac{L}{d}\right)^{0.34}$ according to VDI 2230 standard

ΔL_s the elongation due to strain hardening of the joint surfaces

d the screw nominal diameter

L the useful length between plates

Similarly, we obtain $\Delta F_{L_c} = \frac{\Delta L_c}{\delta_v + \delta_p}$ with ΔL_c the elongation due to creep.

If $F_0^- < F_{0,min}$, there is a possibility that the tightening will be below this minimum accepted value, and therefore the risk of the assembled parts coming loose, or worse sealing. Axial forces could also be poorly filtered, and the risk of spontaneous unscrewing would not be negligible.

In case $F_0^+ > F_{0,max}$, the preload may be too high to ensure the mechanical strength of all the components in the assembly.

Spontaneous unscrewing is thus characterised by the relation $F_0^- < F_{0,min}$, as defined earlier.

Finally, when tightening, we can choose a maximum tightening level, i.e. ask for $F_0^+ \equiv F_{0,max}$.

In this case, the non-loosening condition $F_0^- > F_{0,min}$ can be:

$$F_{0,max} - F_{0,min} > F_0^+ - F_0^- \quad (2.6)$$

To characterise loosening, Zarwel (7) uses Thomala's method to determine whether a screw can loosen, by comparing it to a beam.

Indeed, based on Euler and Bernoulli's theory of beams, the screw is compared to a beam embedded at one end. The maximum displacement possible before the screw loosens is then:

$$\delta = \frac{F_t \cdot L^3}{3 \cdot E \cdot I} \text{ or } \delta = \frac{F_t \cdot L^3}{12 \cdot E \cdot I} \quad (2.7)$$

Depending on whether the screw is assimilated to a beam built-in at one end or both respectively.

Using Timoshenko's theory on thick beams, we can add the shear component of the displacement. Zarwel also adds a third experimental term called "thread slip" to correspond to the results he got for his loosening curves.

$$\delta_{crit} = \frac{\mu \cdot F_0 \cdot L^3}{3 \cdot E \cdot I} + \frac{\mu \cdot F_0 \cdot L}{G \cdot S_{eq} \cdot k} + \text{thread slip} \quad (2.8)$$

With:

δ_{crit} the threshold displacement of the screw head before it loosens

μ the global friction coefficient for the threads and the screw head

F_0 the screw preload

F_t the tangential external load

L the useful length between plates

E the Young modulus for the screw

I the second moment of area for the screw

G the shear modulus for the screw

S_{eq} the equivalent resistant cross-section

k the shear correction coefficient for a cylinder

These 3 terms represent the bending of the screw, its shearing, as well as slight slippage in the screw threads, which leads to additional movement of the screw head.

This relation takes into account the geometry of the screw and no longer the external forces (included in the displacement of the head). Correlating unscrewing with the displacement of the screw head can be risky, and requires precautions before being used in a more complex model such as ours.

2.4.2. Numerical studies of the various models

Several numerical studies of this phenomenon have been carried out under different conditions, with the aim of refining or even validating the analytical models, after correlation with the experimental models. They were mainly carried out on the loosening of a single screw, in order to isolate its behaviour, while optimizing the results thanks to a finer mesh. Indeed, for numerical models modelling the threads, this characteristic will be decisive in understanding the loosening, hence the need for a fine, suitable mesh.

Thus Zarwel (7) models a single preloaded screw on an assembly of parts subjected to cyclic transverse loading obtained by forcing one of the two parts to move relative to the other.

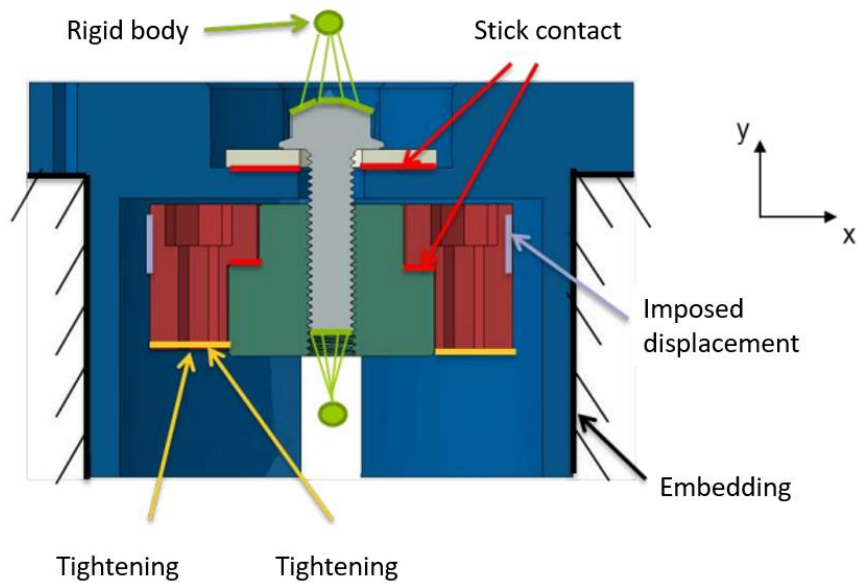


Figure 12 : Zarwel's model for a screw loosening

He then obtains the drop in preload in the screw as well as the rotation of two parts of the screw during the loading cycles.

Loosening – load and rotation

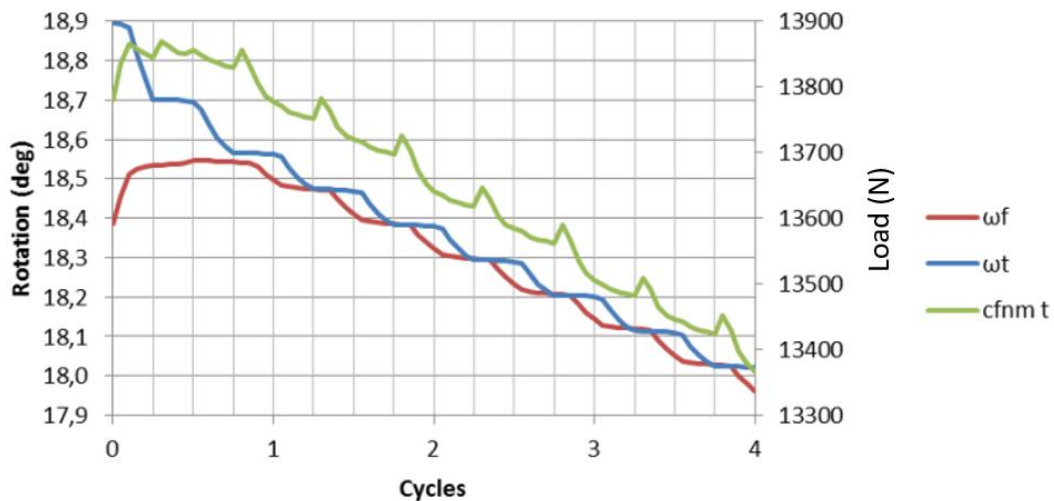


Figure 13 : Unscrewing of the assembly obtained for the previous configuration

From this unscrewing curve as a function of cycles, some researchers define spontaneous unscrewing as soon as it reaches 0.03° of rotation per cycle during the first 10 cycles, or any other steady given value since a slight tension deficit is inevitable due to creep. It is also clear that the screw load is related to the screw rotation.

He also measures the under-head slip as a function of the screw head deflection, a parameter that will be used to correlate the simulation and analytical calculations seen above in paragraph 2.4.1 and which validates the local slippage theory.

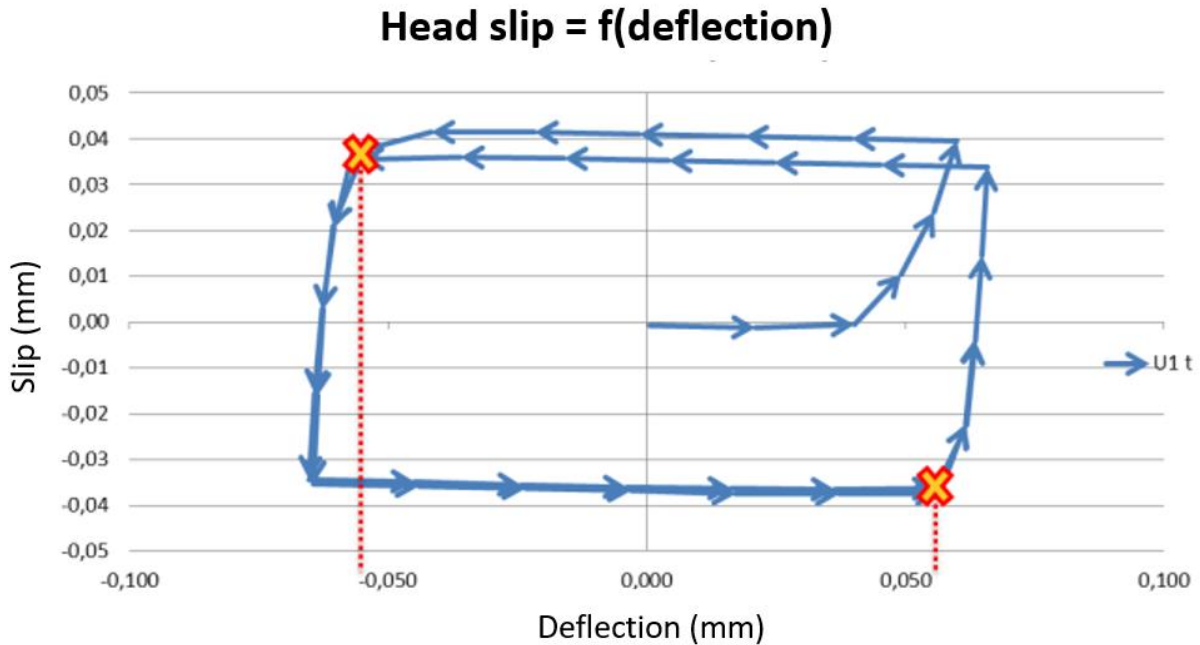


Figure 14 : Appearance of under-head slippage during screw bending

For her part, Ksentini (8) models the behaviour of a bolt whose preload holds in place two plates whose relative displacement is also imposed and sinusoidal.

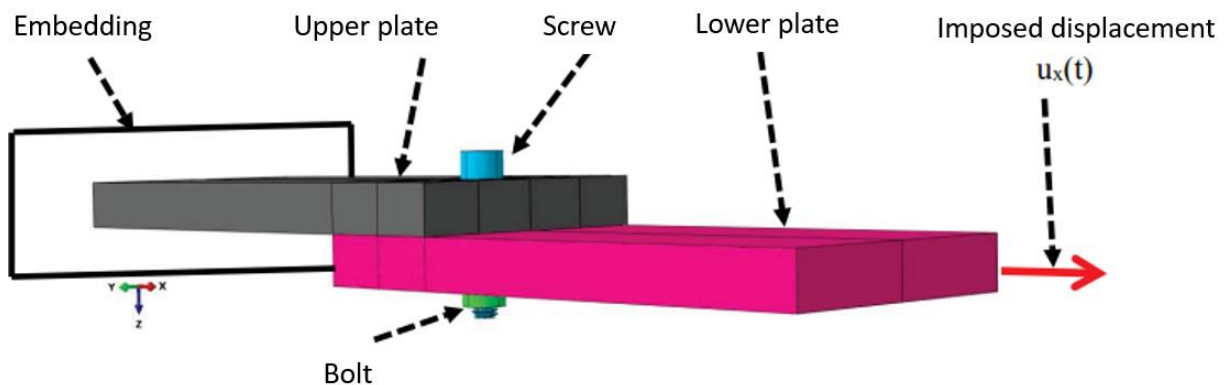


Figure 15 : Model of 2 plates maintained by a bolt

She then obtains the loss of preload and the relative rotation of the screw and nut as a function of time.

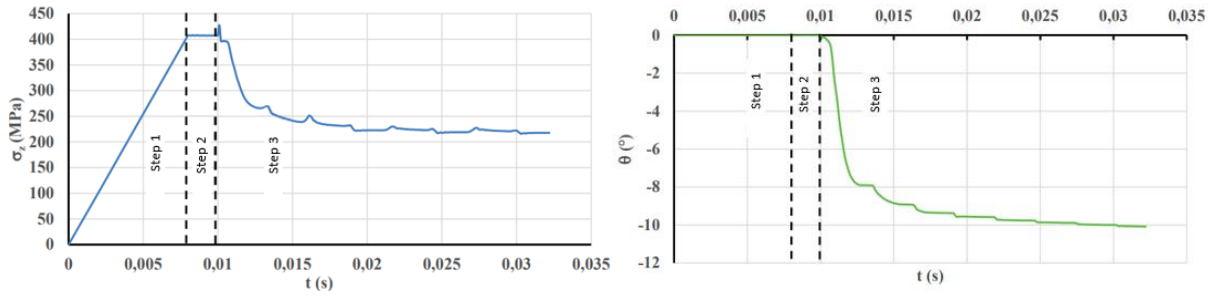


Figure 16 : Axial load in the screw and rotation of the nut in relation to the screw

Steps 1, 2 and 3 correspond respectively to the pre-tensioning of the nut, its stabilisation and the sinusoidal movement of the plate.

All these results for a single bolt can be compared with our case of a bolted assembly, without losing sight of the difference with our case involving several screws and non-planar plates. It would therefore be inappropriate to simply transfer the above results to our case study.

However we notice the importance of screw deflection in the loosening process, displaying the possible use of Thomala's method to predict loosening.

Manoharan (9) is modelling 2-bolt bolted assemblies and stimulating a particular side of his assembly. He then studied the influence of the distance between these two bolts, and the impact of the assembled material on the loosening of the bolts.

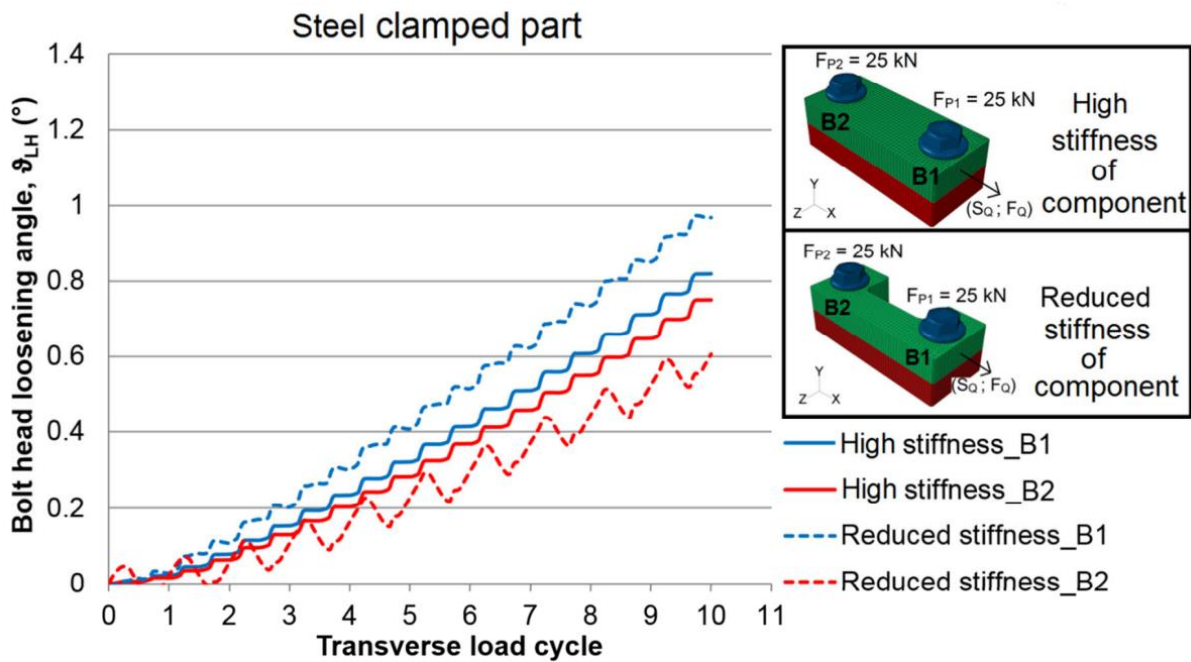


Figure 17 : Loosening of 2 bolts with different stiffness

Two conclusions can be drawn from these results:

- As the displacement stress is applied on the side of bolt 1, the loosening of this bolt is greater than that of bolt 2, and the assembled plates have absorbed some of the energy during the transfer of forces from bolt 1 to bolt 2
- Higher stiffness plates mean greater absorption of the external forces, which increases the loosening range of the various bolts.

He also carries out simulations for different distances between the bolts, i.e. 4 and 7 times their diameter.

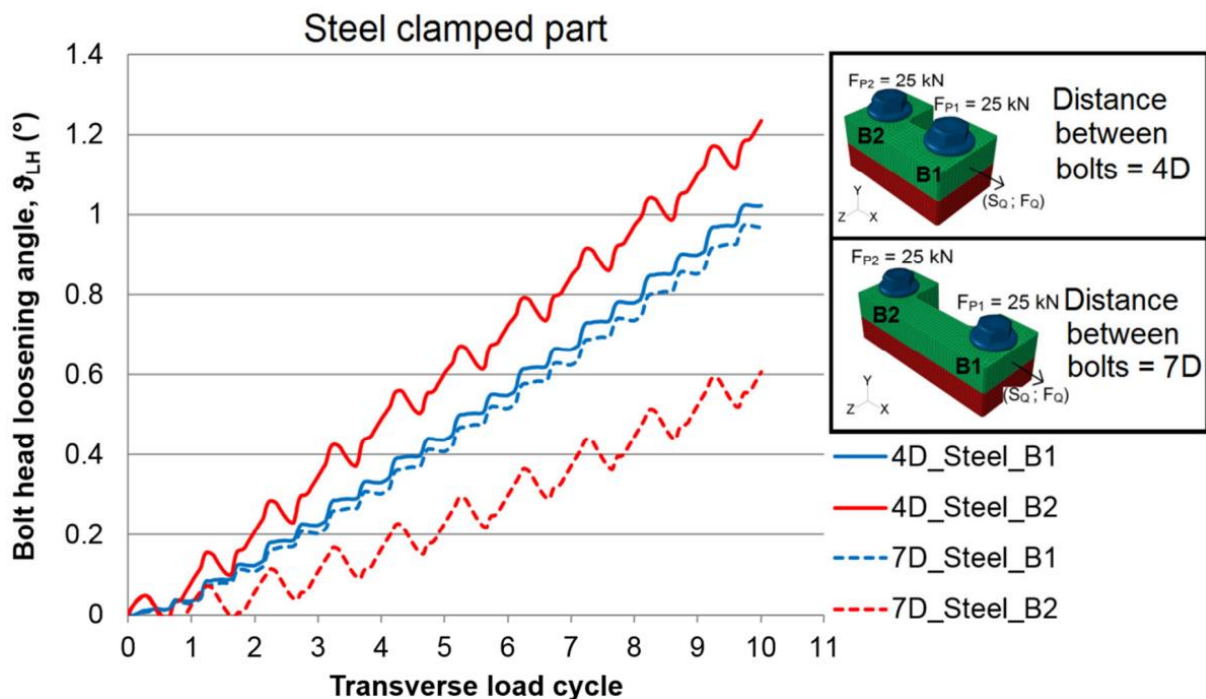


Figure 18 : Influence of bolt spacing

Strangely, the distance between the two bolts has a different effect on loosening depending on their distance apart. It should be clear that bolt B2 loosens less whatever the distance, but it is not the case for a distance equal to 4D. However we clearly notice the impact of the distance between the bolts which can play an important role.

2.5. Previous experimental studies on loosening

In order to validate the analytical formulations and numerical modelling, it is necessary to carry out loosening tests and measurements in parallel to correlate these three aspects.

2.5.1. Experimental studies using 1 screw

Most of the tests are reproductions of Junker's test with a bolt, the diagram of which is given in part 2.3.3.

This machine consists of two parts joined by a tight bolt. A motor imposes a sinusoidal transverse movement on a plate, of a given amplitude and frequency. Sensors are added to the system to measure the loss of preload during loosening, as well as the rotation of the nut relative to the bolt. As this is the test that is widely modelled in the simulations, it is possible to compare the different results obtained.

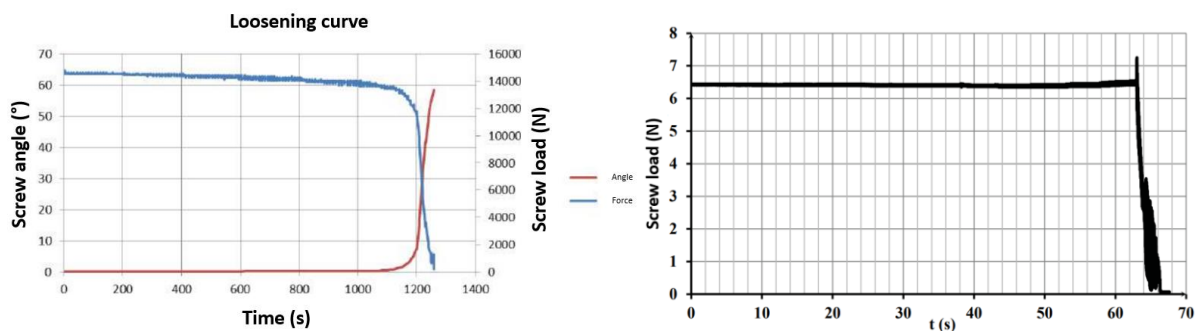


Figure 19 : Junker test loosening curves by Zarwel and Ksentini

Although the set-ups in the literature have different initial conditions, they indicate an overall similar behaviour in the loosening of the bolts as shown by the previous curves; with an initial phase of localised slip, followed by complete slip with a significant loss in pretension. By varying the various parameters of the assemblies, it was also possible to determine their impact on these loosening curves, such as the length of the threaded part, the material of the parts and the screw, and the friction coefficient at the joint surfaces.

Hence Zarwel and Ksentini carried out several studies using other friction values, preloads, screw lengths, materials and surface treatments.

2.5.2. Experimental study using 2 screws

Ksentini (8) also carried out tests with 2 bolts, which are more representative of our wheel screwed assembly containing 4 of them.

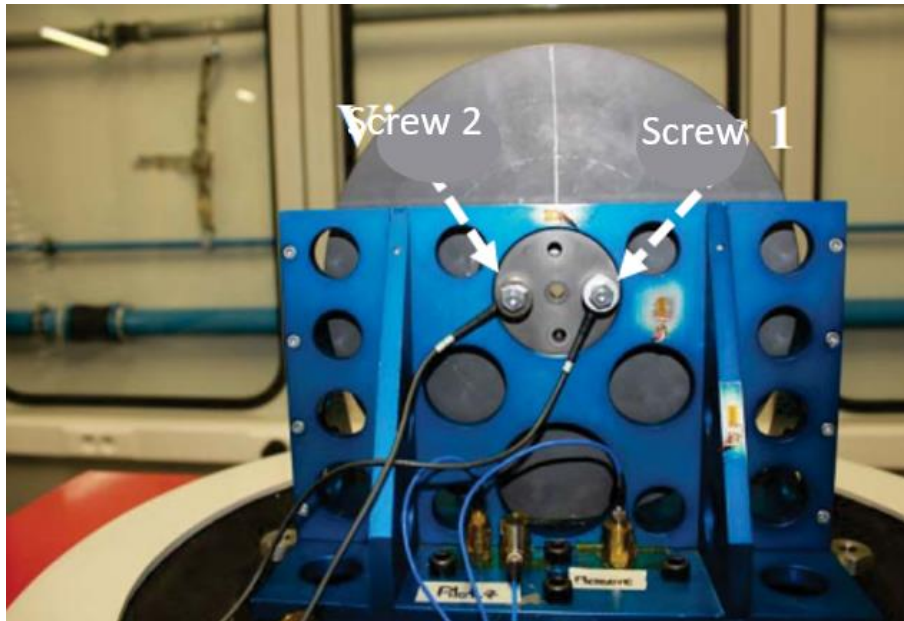


Figure 20 : Bolted assembly with 2 bolts

She then mounts a mass fixed by 2 bolts whose relative positions can be modified, as shown in the photo of the assembly in Figure 20. An electric motor imposes a vertical displacement on the mass, as in Junker's previous tests.

She also compares her results with those from the 1 bolted assembly in order to determine the impact of their number and position.

Overall, the loosening of the connection with 2 bolts would correspond roughly to the loosening with a single bolt, but with the forces doubled. This is contrary to the simulations carried out by Manoharan (9), unless the plates used in his experiment were very stiff.

With regard to the positioning of the bolts with a vertical load, horizontally positioned bolts (as in Figure 20) are less resistant to loosening than when they are arranged vertically, in the same direction as the load. However vertical bolt the closest to the source of the load loosens more than the bolts in the horizontal position.

2.6. Influence of assembly design on loosening

This part of the literature review focuses on changing the design of conventional bolted joints in order to reduce loosening. However, the literature is largely focused on assemblies of 2, flat, parallel plates; the documents studied here report only minor changes with a conventional assembly.

Some other parts of design optimization were already tackled in part 2.4.2, the following section contains the other interesting changes I found in the literature.

2.6.1. Shape of the assembly

The shape of the joint and the position of the bolts in relation to the imposed displacements can have an impact on the loosening of the bolts. Manoharan (9) showed that the distance between a bolt and the stimulus could vary the loosening, in particular from the energy absorbed by the material. Shifting the imposed movement from the bolt axis also helps reduce loosening thanks to the elasticity of the materials, which reduces the displacement of the plates at the bolts.

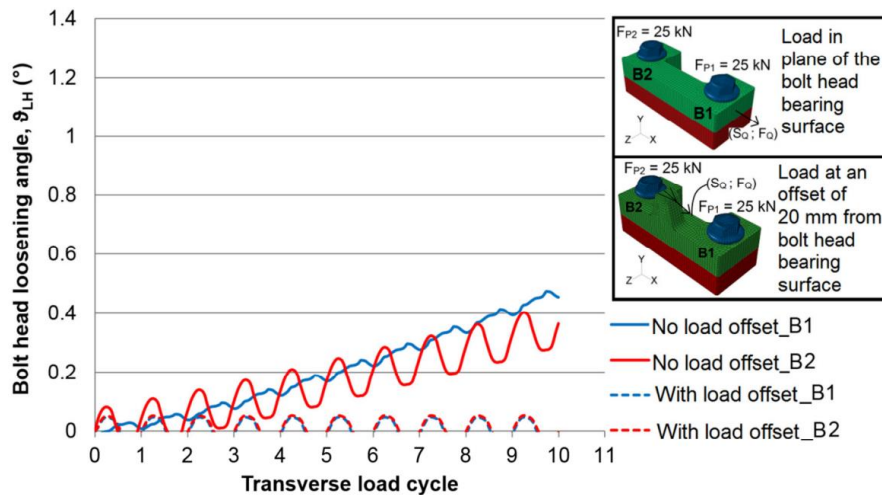


Figure 21 : Bolts loosening with and without shifting the load axis

2.6.2. Assembly parallelism

Although most studies have been carried out on two plates assembled completely parallel, whether at the bolt or further away, non-parallelism has been studied in a few specific cases. It is difficult to draw general conclusions from this phenomenon with respect to loosening. Yang and Nassar (10) as well as Bin Yang (11) consider that two non-parallel plates increase the resistance to loosening, whereas Sawa (12) considers that it's the case of assemblies with parallel faces which is the least conducive to loosening.

2.6.3. Assembly flatness

In a bolted joint, it is necessary to maintain contact pressure between the assembled parts. This pressure not only ensures that the assembly is watertight, but also distributes the forces on the structure.

In a flat plate assembly, the pressure is distributed according to the Röscher cone (13), approximated around 45° from the fastener to the joint between the parts as shown in Figure 22:

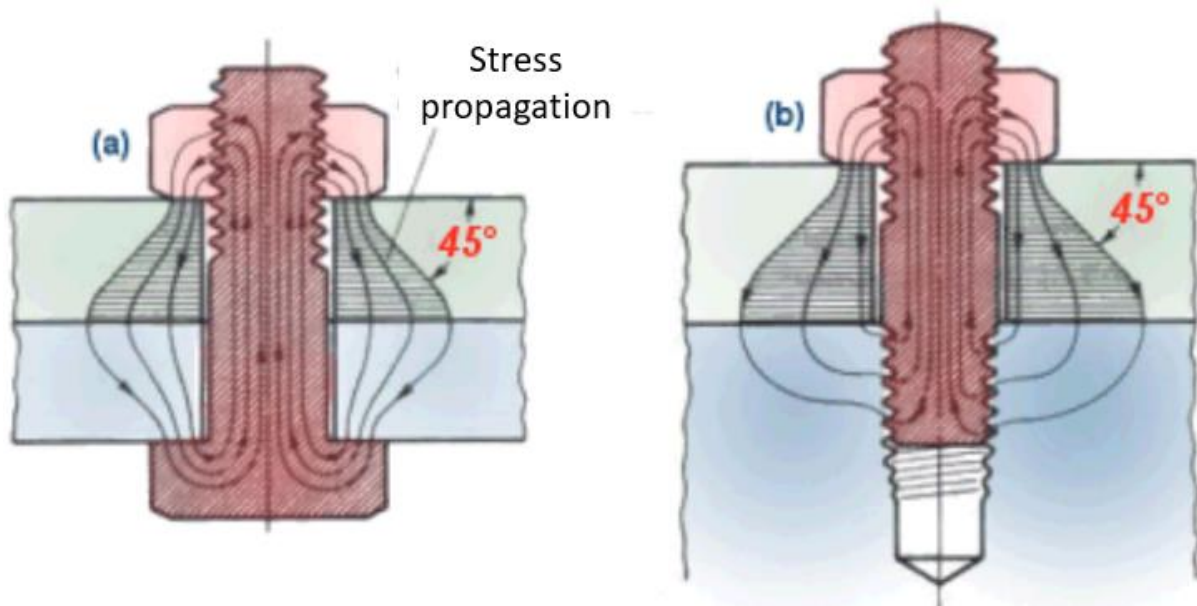


Figure 22 : Stress propagation in the plates

In our case, the interface at the joint surfaces is not flat but distorted, which may influence pressure distribution, preload and the risk of loosening. In fact, the force transmitted by the tightening of the screw to the plates is probably only absorbed by a smaller surface area than in the case of flat plates where the pressure is distributed at 45°.



Figure 23 : Cross-section of the parts clamped by the screw

2.7. Previous work

In order to carry out some of the numerical calculations, an Abaqus finite elements model was available for the study. It contains the main parts of a wheel assembly, including the hub, rim and 4 assembled bolts.

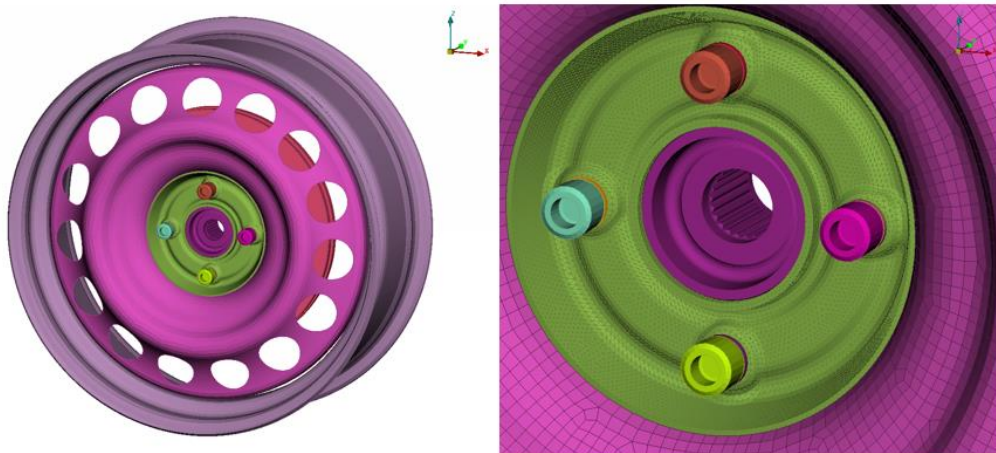


Figure 24 : Meshed model of the wheel (Abaqus model)

This 1.5 million elements model contains both volumetric and surface meshes, depending on the parts.

The materials used are mainly represented by elastoplastic models. It was also necessary to take into account the friction coefficients between the various parts in contact, as they are of prime importance in this loosening study.

Concerning the screws, their preload is modelled without a nut, by a preload section to which the tightening force is applied. The other forces applied are the input forces on the wheel, in order to model the load.

For the boundary conditions, the hub is embedded and the other parts are connected by contact.

Using this model, we can measure various results:

- The pressure and displacement fields within each part
- The screw bending caused by the load
- The plastic deformations of the parts
- The slip fields which are particularly useful for obtaining the threshold displacement studied in part 2.4.1.
- Any other mechanical parameter from Abaqus if necessary

2.8. Literature review critique

The previous section describes various studies on screw connections, an area that is very present in current mechanics research. Although they are varied and extensive, none of them has really dealt with a subject directly applicable to our project. In fact, these studies constitute barriers that require further research into loosening.

The numerical models studied are mainly flat assemblies with parallel plates joined by a single bolt. This research is therefore quite different from the case we are interested in which consists of non-planar plates joined by several bolts. It could therefore be dangerous to try to extrapolate all these results and conclusions to our model, or even to attempt to compare them.

Experimental models are no more representative either, and stop at 2 screws, ignoring the impact of the number of screws and their relative positions in the assembly.

Finally, analytical models cannot take into account all the stresses at contact interfaces, in particular because of localised sliding, in addition to the multitude of contacts and therefore stresses to be taken into account.

These three points underline the research and innovation interest of this wheel design optimization project, especially as the design optimization aspect was not greatly researched either, apart from certain material properties.

However, this literature review still granted us with interesting topics to take inspiration from:

- Thomala's method could predict loosening, but the theory of localised slip also states that loosening occurs when the slip state changes from localised to general slippage for the planar assemblies described earlier, which could be another possibility to predict loosening
- The formula of $F_{0,min}$ as well as the relation (2.6) give a good insight at what parameters should be changed in order to reduce loosening, as well as other parameters specifically studied in the literature
- The few studies made on design optimization against spontaneous loosening bring even more confidence in the previous point with the parameters to change for our optimization

3. Numerical loosening study

3.1. Cobra V6 loosening comparisons

CobraV6 is a software that enables the user to model simple bolted assemblies, in order to gather some data on the various mechanical characteristics of this assembly, including the potential self-loosening.

Indeed, Cobra uses the Kellerman and Klein equation (2.4) and the mechanical parameters of the assembly $F_{0,max}$ and $F_{0,min}$ to get to the equation (2.6) shown in part 2.4.1.

By representing the possible pretension force applied on the screw with a blue line, and the admissible preload for the mechanical assembly, in order to stay in the $[F_{0,min}; F_{0,max}]$ interval in green, a correct assembly with not risk of loosening should look like this:

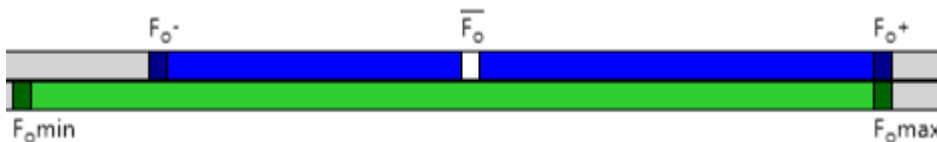


Figure 25 : Cobra results for a non-loosening assembly

However, there is no uncertainty on the torque, and the friction coefficient is set in the simulation.

Therefore the tightening preload is exactly $\overline{F_0}$, and the only equation that needs to be satisfied is $F_{0,min} < \overline{F_0}$ to avoid loosening.

Also, the value $\overline{F_0}$ is equal to 2659N. It corresponds to the F_0^+ value equalled to $F_{0,max}$ for the mechanical safety of the assembly, minus the uncertainty of tightening due to the torque and the friction coefficient.

The model used to correspond to the assemblies which Cobra was able to do only consisted of 2 plates and 1 screw in the middle. The geometrical parameters are give below. Concerning the material properties, both plates and the screw had a Young's modulus of 210GPa and Poisson's ratio of 0.285. It was necessary to stay in the elastic domain since Cobra could not handle plastic deformation.

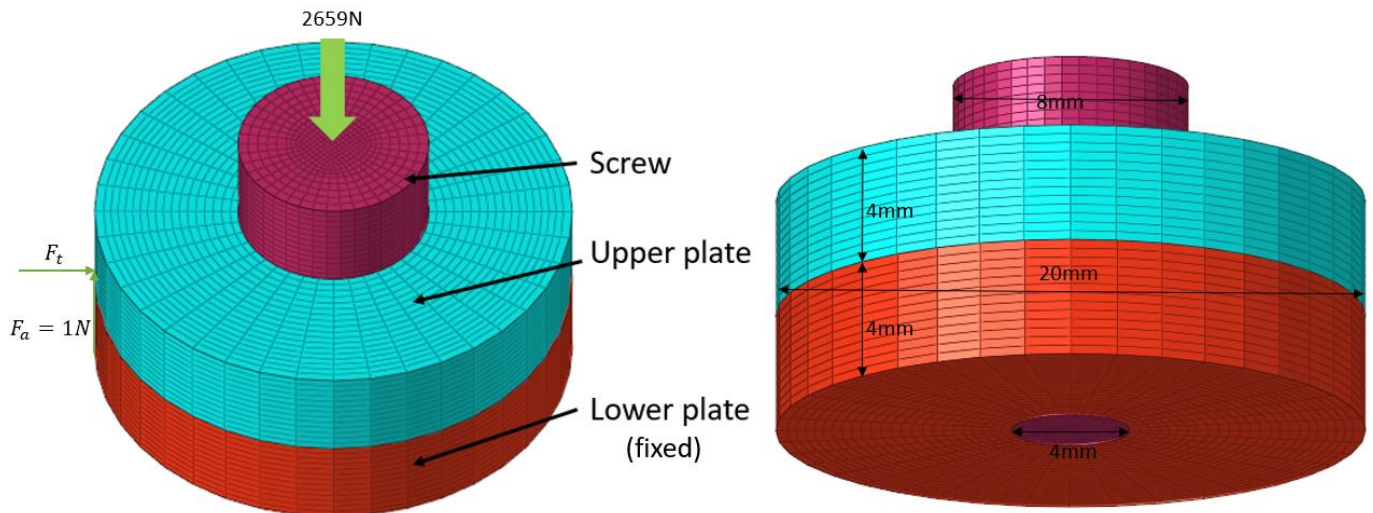


Figure 26 : OptiStruct model of the simple Cobra assembly

Concerning this model, the contact between the plates was driven by a Coulomb contact using a dynamic and a static friction coefficients. The same contact rule was applied to the interface between the head of the screw and the upper plate. The lower plate was fixed as well as the lower half of the screw body.

Eventually, 2659N of pretension were applied to the screw according to Cobra software, in order to match the theoretical F_0^+ value with $F_{0,max}$. An axial load and a tangential load were also applied to the upper plate.

The goal of this study is to determine the start of self-loosening with parameters inside OptiStruct, that is to say noticing the changes in OptiStruct which have the assembly change from no loosening to self-loosening, using the criteria given by Cobra.

To reach the self-loosening stage, it is necessary to increase $F_{0,min}$ past F_0^- . Thus I increased the tangential load on the upper plate. Ideally, to observe any change in the bolted assembly when going past this stage, we try to run several models before and after this stage, with multiple ones when $F_{0,min}$ is very close to F_0^- .

The first step to use the Cobra software was to gather the forces F_{ax} and F_t applied on the screw, because these can be different from the initial forces applied on the upper plate. I did so by changing the 3D screw with a 1D beam of 1 element, hence I got the axial load and the shear load to be entered in Cobra. After getting this Cobra model, I could set it up with different loads to compare the stages before and after reaching self-loosening.

After studying 16 different load cases with a different tangential load on the plate, I could compare the results I got and plot them with respect to the external (tangential) load.

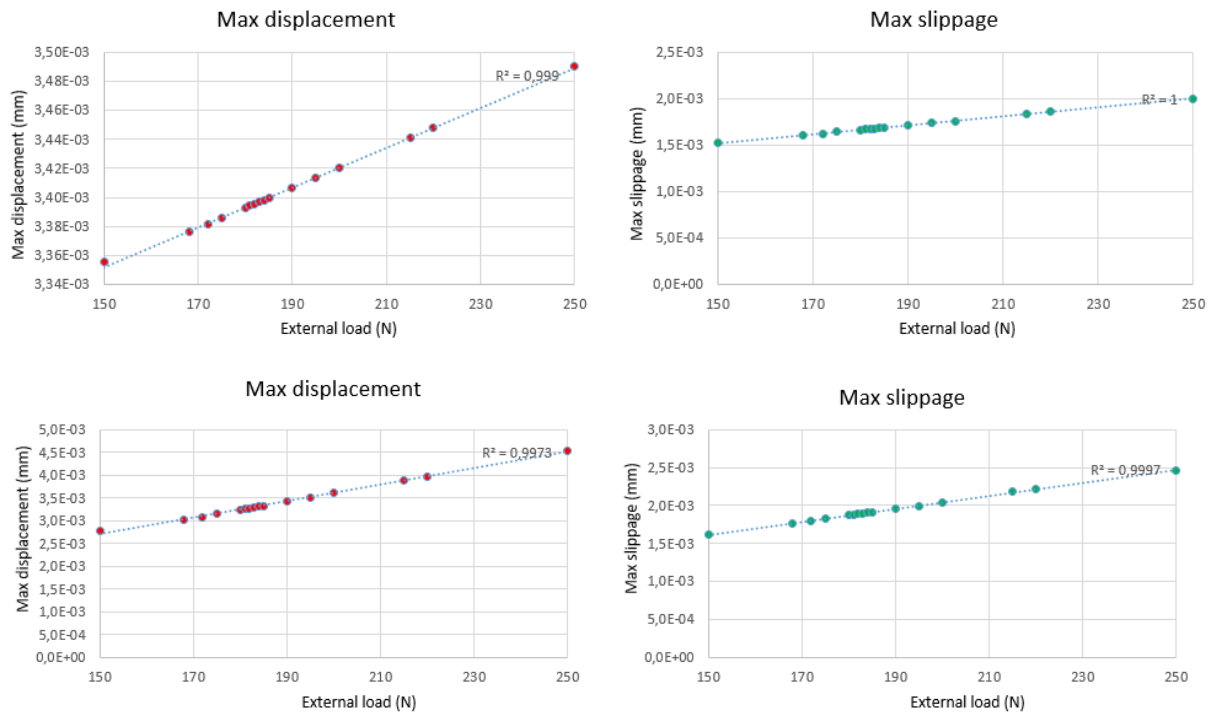


Figure 27 : Results of the 16 models on the screw (top) and the upper plate (bottom)

These results show the maximum displacement (in red) and the maximum slip distance (in green) for the screw and for the upper plate, with different loads on the plate. Unfortunately, the R^2 close to 1 on each of these curves shows that the different points form a straight line, that is to say the maximum displacement and slippage for the screw and the plate are affine functions of the load, and cannot help differentiate the self-loosening stage from the non-loosening stage.

Similar results were obtained for other output data, and none could help us determine when the assembly reached a self-loosening stage only based on the OptiStruct model.

Moreover, the contact status between the upper plate and the head of the screw remained all the time stuck, even with the Coulomb contact model. However, according to the localised slip theory, the screw head should start slipping from the upper plate just before reaching loosening. This is not what happened with our different models, when none showed any slip between the head and the upper plate, even with an external load supposedly enough to get to self-loosening according to the Cobra results.

More precisely, the model was made so that a large enough external force could have the upper plate leave the lower plate. Indeed, the only contacts were between the head of the screw and the upper plate, and between both plates, thus the only forces preventing the upper plate from leaving the lower plate was the tangential force given by the Coulomb contact. These solids are deformable, hence the simple Coulomb theory is not enough to tell whether the screw pretension will have the upper plate stay close to the lower plate despite

the tangential external load. However, a large enough tangential load (higher than the 180N shown here) could have it slip.

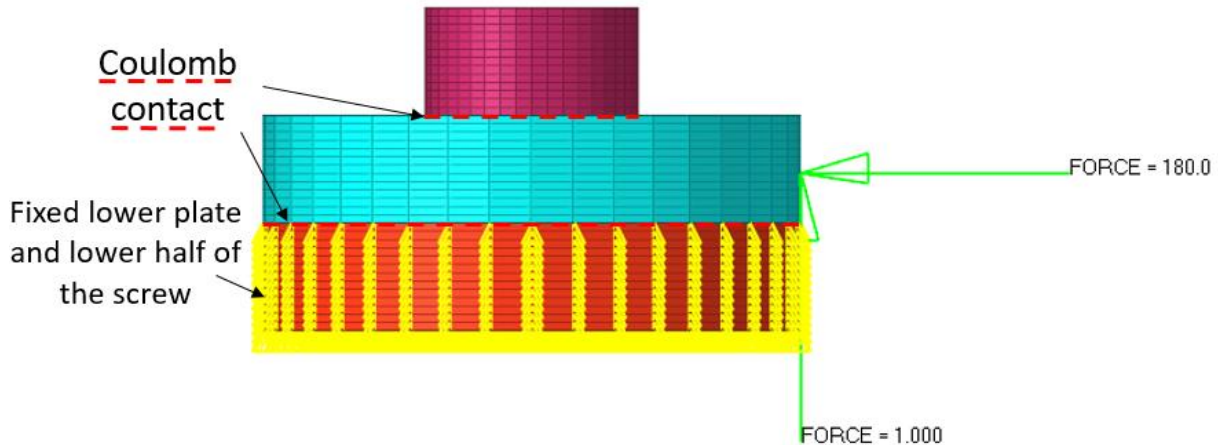


Figure 28 : Contacts on the simple OptiStruct model

The previous loads did not exceed 250N of external tangential force. However, when increasing this load to 501N, the head of the screw split up into one half slipping with the upper plate, and the other half stuck with Coulomb's frictions. It is what was explained in the local slippage theory part 2.3.1.

Generally speaking, when a load is applied to the bolted assembly, the parts in contact may start slipping despite the pretension, especially the screw head with the upper plate. This slip, which initially is only local slip, increases loosening, which increases the slip area to end up in a complete slippage state where the screw head completely slips with the upper plate. In our case, we estimate the transition between local slippage and complete slippage when the slip region on the screw head exceeds 50%. This state is reached when the external load applied to the plate is 501N, for our loosening case of 2659N of screw pretension. Therefore we will consider loosening at this state when using Thomala's method.

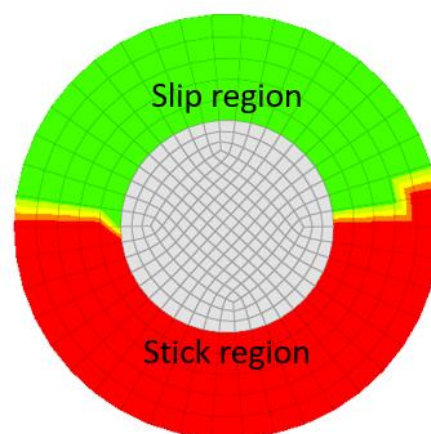


Figure 29 : Screw head contact with the upper plate at 501N of external load, slip (green) and stick (red) regions

3.2. Thomala's method

Another method to determine whether an assembly will loosen is Thomala's method, as explained in part 2.4.1. Indeed, Thomala compares the displacement of the head of the screw to its theoretical displacement in "normal" conditions. If the head moves more than it should according to the model after the external loads are applied, it means the assembly is likely to loosen.

First of all, it is necessary to correct the relation (3.8) given for one single bolt. Indeed, we have to keep in mind this relation was found with the approximation of a beam fixed at one end. However, this approximation can be corrected depending on the conditions of the screw.

If the bolt is supposed to be fixed at one end, we can keep the Bernoulli's component of the critical displacement as $\delta_{crit,E.B} = \frac{\mu.F_0.L^3}{3.E.I}$, but if it is longer, it is better to suppose the beam is built-in at both ends, and change this component of the critical displacement to $\delta_{crit,E.B} = \frac{\mu.F_0.L^3}{12.E.I}$.

However, the length of the screw or the beam has to be compared to its diameter to know whether to screw can be supposed thick enough to add Timoshenko's component, since the beam can be thicker than what Euler and Bernoulli's theory could include. In that case, we add Timoshenko's component for the shear of the beam $\delta_{crit,T} = \frac{\mu.F_0.L}{G.S_{eq}.k}$.

Moreover, the numerical models have no play between the threads and the plates, or it is simply modelled by no contact between the screw body and the upper plate in our case. Therefore we cannot keep the "thread slip" in the critical displacement formula.

Finally, the difference between a beam fixed at one or both ends is mainly made by the ratio L/d with L the length of the screw and d its nominal diameter. When $L/d > 3$, we can consider the screw to be fixed at both ends, and we can consider it only built-in at one end when $L/d < 1$. When $1 < L/d < 3$, it is necessary to take the angle of the screw into account, so that it is possible to differentiate the case where the beam is built-in at one or both ends. This angle corresponds to the bending of the screw after the external loads are applied.

To summarize, the general relation for the critical displacement will take into account both Euler and Bernoulli and Timoshenko's components for more accuracy. In that case, the numerical formula will simplify the relation (3.8) to:

$$\delta_{crit} = \delta_{crit,E.B} + \delta_{crit,T} \quad (3.1)$$

With:

δ_{crit} the critical displacement of the screw

$\delta_{crit,E.B} = \frac{\mu.F_0.L^3}{3.E.I}$ for beams fixed at one end

$$\delta_{crit,E.B} = \frac{\mu \cdot F_0 \cdot L^3}{12 \cdot E \cdot I} \text{ for beams fixed at both ends}$$

$\delta_{crit,T}$ for the shear component

In the case presented part 3.1, the diameter of the screw is 4mm, and the length of the screw body that is not fixed to the lower plate also is 4mm. Thus the ratio L/d is between the two Euler and Bernoulli's cases for the critical displacement. The correct case has to be determined based on the angle of the screw:

If the angle formed by the play in the thread is higher than the angle of the screw when it is bent by the external loads, the case considered is the same as if $L/d < 1$. However, our model has no play between the screw body and the plates. Therefore the displacement component used will be the one for a screw fixed at both ends. This is also verified by the displacement of the screw with respect to the height position in the screw body, which clearly matches more the curve of a beam fixed at both ends instead of only one.

The critical displacement used in this model will be:

$$\delta_{crit} = \frac{\mu \cdot F_0 \cdot L^3}{12 \cdot E \cdot I} + \frac{\mu \cdot F_0 \cdot L}{G \cdot S_{eq} \cdot k} \quad (3.2)$$

To measure the corresponding displacement of the screw in the simulation, it is necessary to keep the same kind of hypothesis as the ones made to get to equation (3.2). Hence, the length taken into account will be the length of the screw between the fixed lower plate and the bottom of the screw head, because the lower part of the screw which is fixed has by definition 0 displacement, and the head of the screw has no direct load applied to it since it is above the upper plate. Obviously, the diameter used for I , G and S_{eq} is the diameter of the cylinder since the threads were not represented in this model. The main geometric parameters are summarized in the image below:

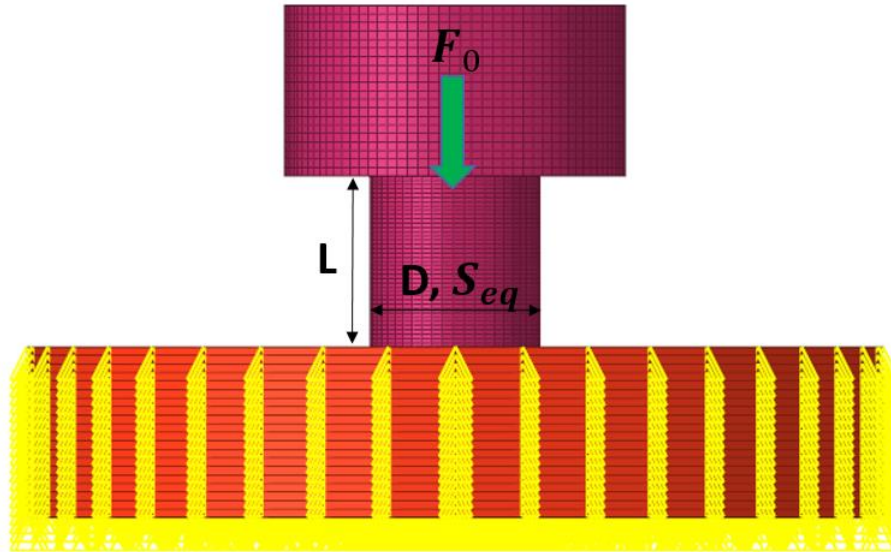


Figure 30 : Geometric parameters for the simple Cobra model in OptiStruct

When this value is computed, we obtain an analytical critical displacement at $1,78\mu m$.

In addition, to measure the correct displacement of the supposed beam, we need to find the point on the neutral axis at the end of the beam right before the screw head, in the center of this circle section. We also need to solely consider the transverse displacement caused by the external load and not by the tightening.

In the case of 501N tangential load applied on this upper plate, the tangential displacement of this point of the screw reaches $1,777\mu m$.

Therefore, Thomala's method applied to this kind of bolted assembly seems to properly determine loosening according to the previous hypothesis made, contrary to Cobra whose results did not correspond to OptiStruct's results.

4. Wheel model conversion

First of all, in order to optimize the design of the wheel, it was necessary to have it modelled on a computer. Fortunately, we had a wheel model available under Abaqus with the complete numerical simulation. All the parts were meshed, the loads were set on the rim and the hub was embedded.

However, it was not possible to use the Abaqus solver at Segula due to license issues. It was therefore necessary to convert it into OptiStruct from HyperMesh.

The following parts describe how the conversion was made, and checked so that the new wheel model on OptiStruct would be likely to represent what happens with Abaqus. It is also worth noting the version used for HyperMesh was version 2017.2, but other simulations were run later remotely with 2020 and 2021 versions.

4.1. Automatic conversion

Part of the conversion from Abaqus to OptiStruct can be made automatically by the software, using the option “Convert” from the “Tool” menu. This handles the different parts along with their mesh and element formulation, some of the contacts between parts, the external load and some material properties.

The remaining conversion of the model had either to be made by hand or to be deleted if it was not seen as necessary.

4.2. Material properties conversion

Not all the properties of the materials were converted correctly. Hence, I had to convert and recreate the elastoplastic properties for the 4 different materials. The data for Hooke’s law were given, and 2 points were available for the plastic part of the stress-strain curve. This part was not difficult thanks to the information we had and how the OptiStruct solver could do it.

4.3. Membranes conversion

The Abaqus model contained membranes for the 2 shell parts in order to easily post-process the output data. Indeed, usual shell elements have their data calculated at their neutral axis, which may be far from the actual border of the part, even with the shell

assumptions fulfilled. Hence, these membrane parts are stuck to their respective shell parts, but with a shell thickness around 1nm so that the data measured at the edge of the membrane is the same as the one on the neutral axis.

However, OptiStruct could not handle plastic material properties with such membrane components. We hence had to remove these parts and be careful during the analysis of the post-processed data for the shell components.

4.4. Contacts conversion

The conversion of the contacts was the one HyperMesh could do the least well, and a lot had to be revised especially because this is a very critical aspect of the model.

In order to set up a contact between parts in OptiStruct, I needed to both determine the elements and nodes implied in this contact, and define how the contact should be managed.

When it comes to the elements and nodes of the parts in contact, most of them were visible on the Abaqus model, so the conversion could easily be made by hand. It was also useful to reduce some of them to the minimal surfaces possible to reduce the computing time. Choosing nodes or surface elements for the contact depends on how the contact is defined, and which of the contact parts is the slave or the master.

4.4.1. Contact definition

There are several possibilities to define contact between parts. It is possible for the parts to either interact upon contact or to remain in relative position like stuck together.

When the contact is set for the parts to interact upon contact, the contact can be detected following different discretization rules. These rules differentiate Node to Surface and Surface to Surface contact.

A Node to Surface contact discretization requires defining a master set of surfaces and a slave set of nodes, between the parts in contact. The slave nodes are given in the set of nodes, and the master surfaces are defined using the nodes of the main surface as well. The slave nodes are then projected on the master surfaces, and their smallest distance to the surface creates the normal of the surface with the corresponding node. In case no normal projection is detected, the nearest segment is considered the distance between the two parts instead if the angle with the theoretical normal is lower than 30°.

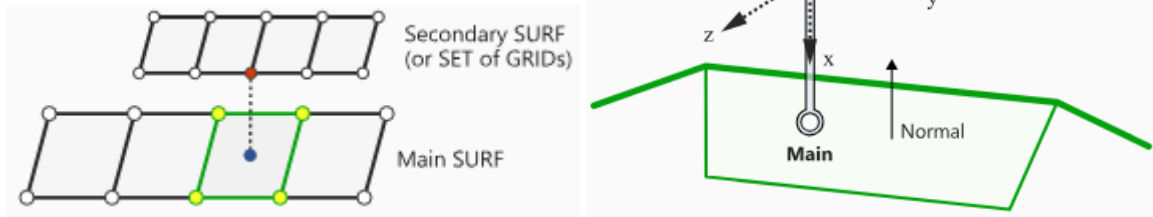


Figure 31 : Node to Surface contact discretization

Once the distance of this normal is smaller than a distance previously specified (search distance), the element is considered to be in contact with the master surface.

A Surface to Surface contact discretization requires defining contact element surfaces for both master and slave parts. The solver creates sample points on both surfaces to compute the distance between them, similarly to Node to Surface contact. The smallest distance between different sample points is considered the distance between the parts, and contact is detected if this distance is smaller than a distance previously defined.

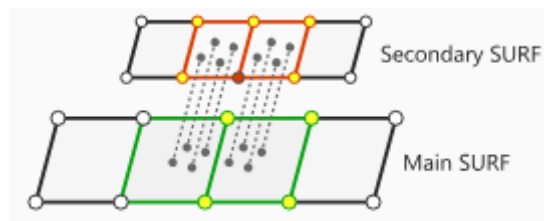


Figure 32 : Surface to Surface contact discretization

Before the contact is determined, OptiStruct also enables the user to adjust the parts theoretically in contact to touch at the beginning of the numerical simulation. In other words, if 2 part meshes are not exactly touching with a zero distance between them, the solver moves the slave part so that the contact is initially detected. This helped get a smoother model despite a complex geometry due to the shape of the parts and the mesh.

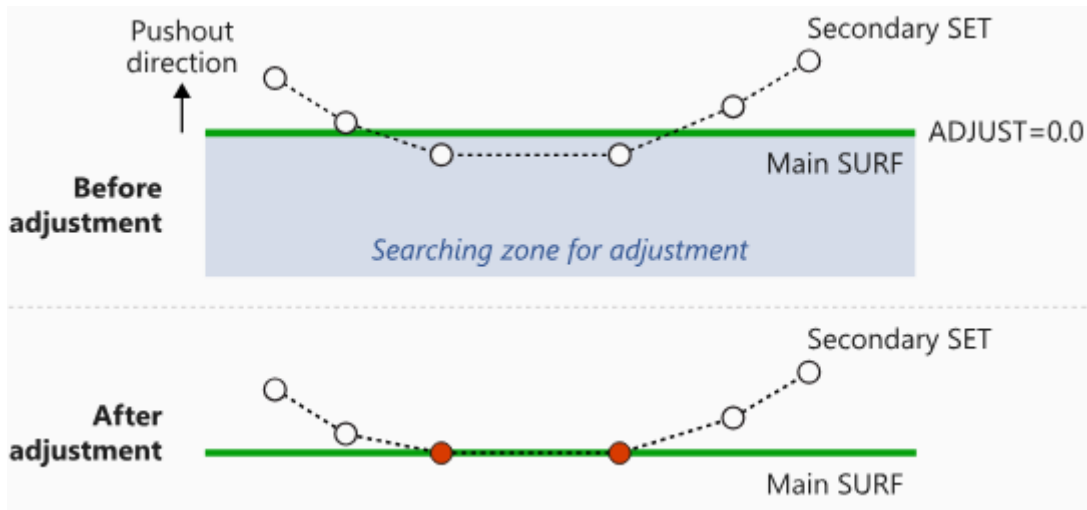


Figure 33 : Adjust parameter for penetration or separation

It was also possible to define the tracking of the contact, choosing between small sliding and finite sliding, sliding being allowed thanks to specific contact properties defined in part 4.4.2. The small and finite sliding matter depends on the potential length of the slip between parts. In our case, deformation was important but the slip was small, hence small sliding was necessary for optimal contact management.

All in all, all the contacts were defined as either tie contact or Coulomb contact with Node to Surface definition and small sliding, with their respective friction coefficient. However, after the first conversion of the model, we noticed an abnormal behaviour of the contact pressure. Indeed, the contact pressure was far above zero in a region where no contact was supposed to happen during the whole analysis.

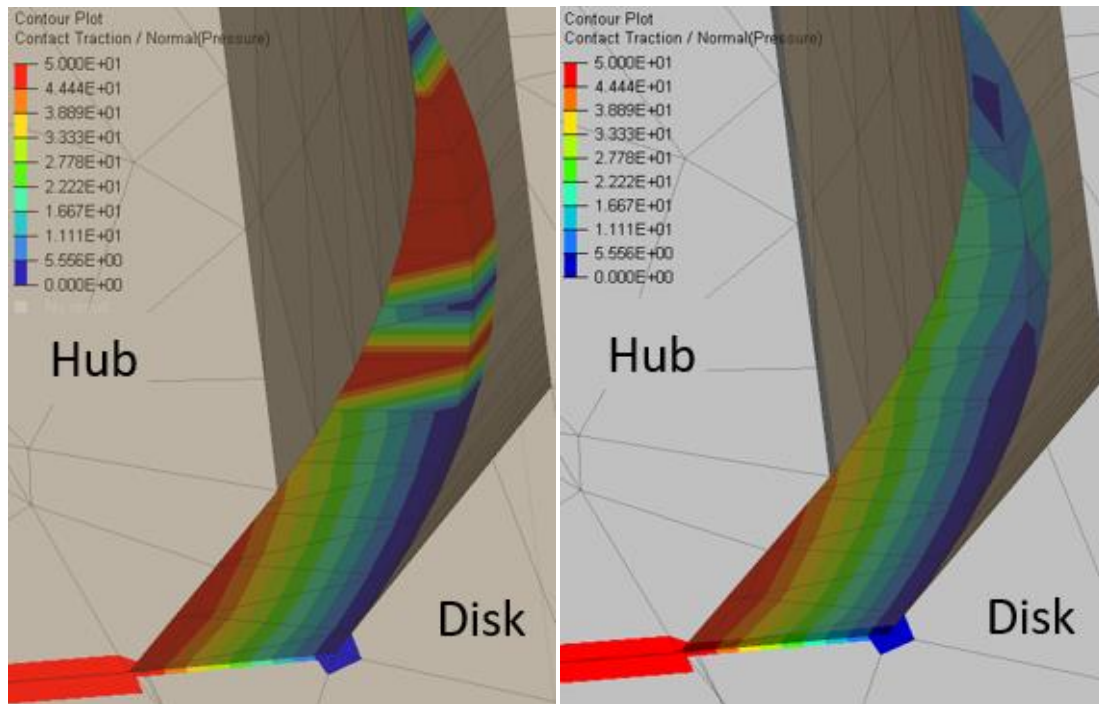


Figure 34 : Contact pressure on the disk in contact with the hub, with n2s (left) and s2s (right) discretization

In this picture, we see can the contact pressure on the side of the hub in contact with the disk. The pressure is given in MPa and can exceed 50MPa for some areas in red. On the left is the model where this contact used Node to Surface discretization, and on the right is the new model with a Surface to Surface discretization.

The reason behind this flaw is the way OptiStruct computes contact pressures. Indeed, the contact pressures are first determined at the face of each element. However, Hyperview only displays the pressure at the nodes such that the average of the nodes gives the surface pressure for each element. Hence, the pressure was above 50MPa in some areas without contact, because some elements on the side of the disk were in contact with other elements of the hub.

This issue was solved using Surface to Surface contact for this interface. We clearly see the value of contact pressure decreased on the side of the disk, as it should.

After a meticulous check of all the other contact interfaces, no other contact pressure was computed out of the contact surfaces, so all the other contacts remained discretized as Node to Surface contacts.

4.4.2. Contact properties

Once the contact is detected, it is necessary to define how the parts will interact together. The different contacts defined in this model either used a Coulomb friction coefficient or tied the parts together.

For the Coulomb contact definition, it was necessary to define the static friction coefficient given in the Abaqus model and allow the possible separation of the parts, meaning a search distance lower than the computed distance between the master and slave components. The dynamic coefficient was equal to the static coefficient by default. The contact properties also enable the contact to be determined from the side of the shell components rather than the neutral axis.

For the stick contacts, it was necessary to tie the bottom of the screws to the hub for the tightening, which was defined between master surfaces of the hub and slave nodes of the screws.

4.5. Model steps conversion

In order to properly run the model, I had to define the different steps, which were not the same as in the Abaqus model. Running this model required only 2 steps with OptiStruct when 3 were necessary for Abaqus.

The 2 steps included 1 step for the tightening of the screws and 1 step for the load of the rim. Both steps were run successively so that the load step kept the effect of the tightening of the screws. The analysis was run with non-linear quasi-static type because HyperMesh v2017.2 did not include non-linear static like the 2021 version. Both steps were ran with this analysis type, and other parameters relating to non-linear analysis.

The first step for the tightening only required redefining the pretension section (in green below) of each screw, slightly below the bottom of the cones, as well as the preload.

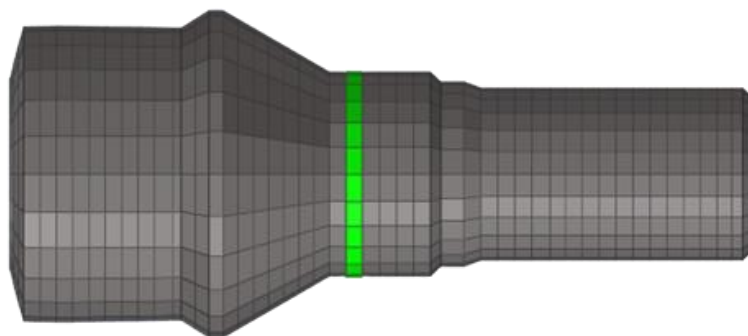


Figure 35 : Pretension section of a screw in green

The second step required to add the different loads on the rim, but the nodes to set these 2 loads were already defined in the Abaqus model for this load case.

4.6. Non-linear static parameters

Running a non-linear analysis with OptiStruct required additional parameters to properly reach the converging solution. Non-linear parameters allowed to specify the initial increment for the simulation as well as the maximum number of iterations before reducing the increment.

I also added specific output card requests to gather data for the contacts of the parts, to help compare with the initial model.

4.7. Mesh optimization for reduced computing time

The mesh was completely converted thanks to the automatic conversion tool. However, this was clearly not optimal, and even before comparing the output results, I noticed the computing time was way too high for any possible later optimization of the model. Indeed, the memory available on my computer was too small, and running the complete model using 32 processors took around 4-5 days. The main reason is the number of elements to consider, increasing as well to a huge number of elements and nodes possibly in contacts.

The initial model contained about 1,5 million elements, mainly for the disk and the hub which were meshed with 3D tetra elements. These two parts are therefore the ones I optimized the mesh. The general considerations to follow in order to coarsen a mesh are what I followed to make a 3D tetra mesh for both parts.

- Trim the geometry to change the mesh using relevant parameters for the number of elements and the bias along trim lines. This enables the mesh not to be uniform, and focus the mesh with smaller elements near the areas of interest. In addition, no big defeaturing was necessary here since the shapes were rather simple.
- Mesh the surfaces with 2D trias elements using the trim lines. The smallest elements need to be focused on the areas with greater stress gradients and highly non-regular geometries.
- Fill the geometry with 3D tetra elements from the trias surface. Moreover, using a quadratic formulation for tetra elements instead of linear formulation helps reduce the stiffness flaw of this formulation.

After remeshing these components, the total number of elements was reduced to about 0,5 million, which highly helped the simulation run in only 2 to 3 hours with the same amount of processors.

4.8. Models comparison

Before comparing both models after the conversion, it is also necessary to keep in mind the initial model made for Abaqus solver was not correlated to any test nor analytical result. This is why the priority for this conversion is to have a model which fits the expected reality as well rather than only trying to perfectly match the results of the initial model. Yet the initial model was not too bad, and getting close results can only be a good sign for the well-conversion of the model.

The main results available concerning the initial Abaqus model were regarding displacement, slip and contact pressure. These are the 3 parameters we will look at in order to compare with our new model.

Because of confidentiality, the numerical values will not be given, but the colored scales can give an overview of the similarities and differences.

4.8.1. Displacements comparison

Since the model is using large displacement analysis, comparing them can give a good insight of the possible differences. We will only view here the displacement of the whole wheel at the end of step 2 (after the load).

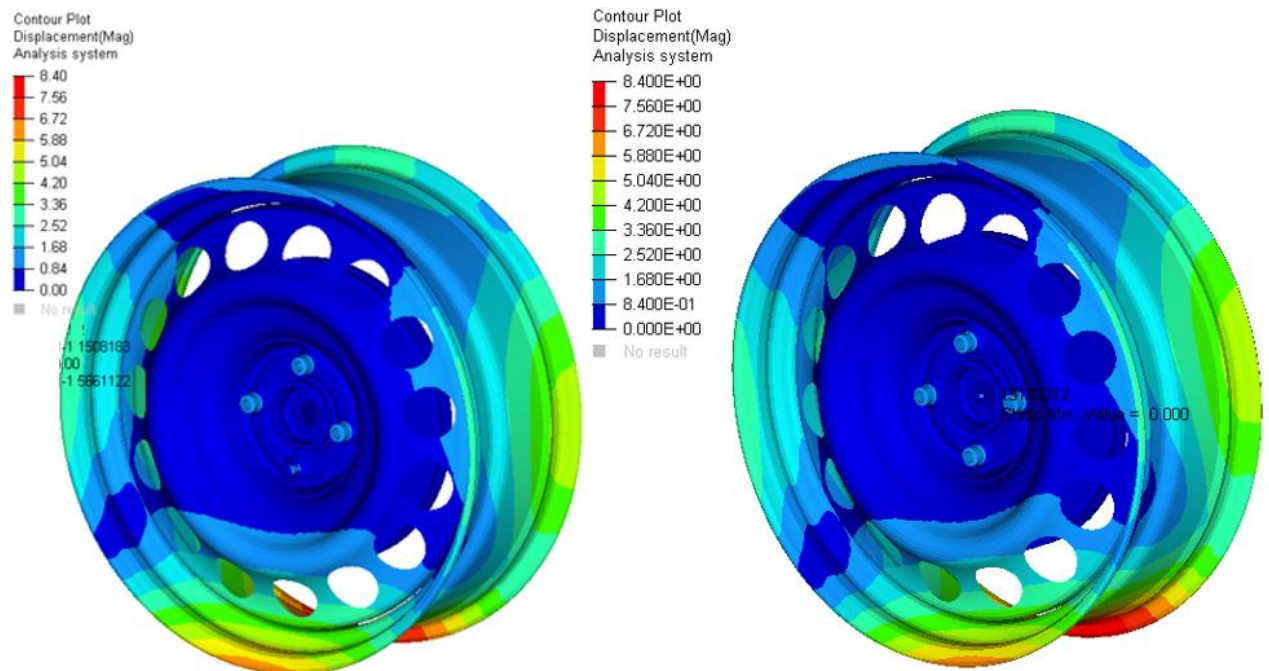


Figure 36 : Displacements of the wheel with Abaqus (left) and OptiStruct (right)

We notice a small displacement of the screws, due to their tightening. The other relevant parts are the 2 red spots at the bottom side of the rim. These parts have higher displacement because it is where the load is applied.

When comparing these models (with this view and others not displayed in this report), we notice no important difference whatever the part. When it comes to matching the displacements, this conversion is a success and no result seems to be far from reality.

4.8.2. Slips comparison

Comparing the slip of parts between the models only concerns the parts where contact takes place. Except for the 4 screws and the middle of the rim, all the other contacts are set using the Coulomb definition and with the same dynamic friction coefficient as the static coefficient. Hence, slip occurs when the tangential force exceeds the normal force multiplied by the local friction coefficient.

The locations where the slip is 0 either mean the slips cancelled, or that no slip ever occurred here.

Among the different interfaces where slip was potentially present, the ones I will compare in this report are between the rim and the disk, and between the disk and the hub, both at the end of the load.

Concerning the slip between the rim and the disk, no major difference is present. Only a small sliding is present on the inner part of the rim, which might be due to the new mesh of the disk. When it comes to the slip values, they seem to be rather similar.

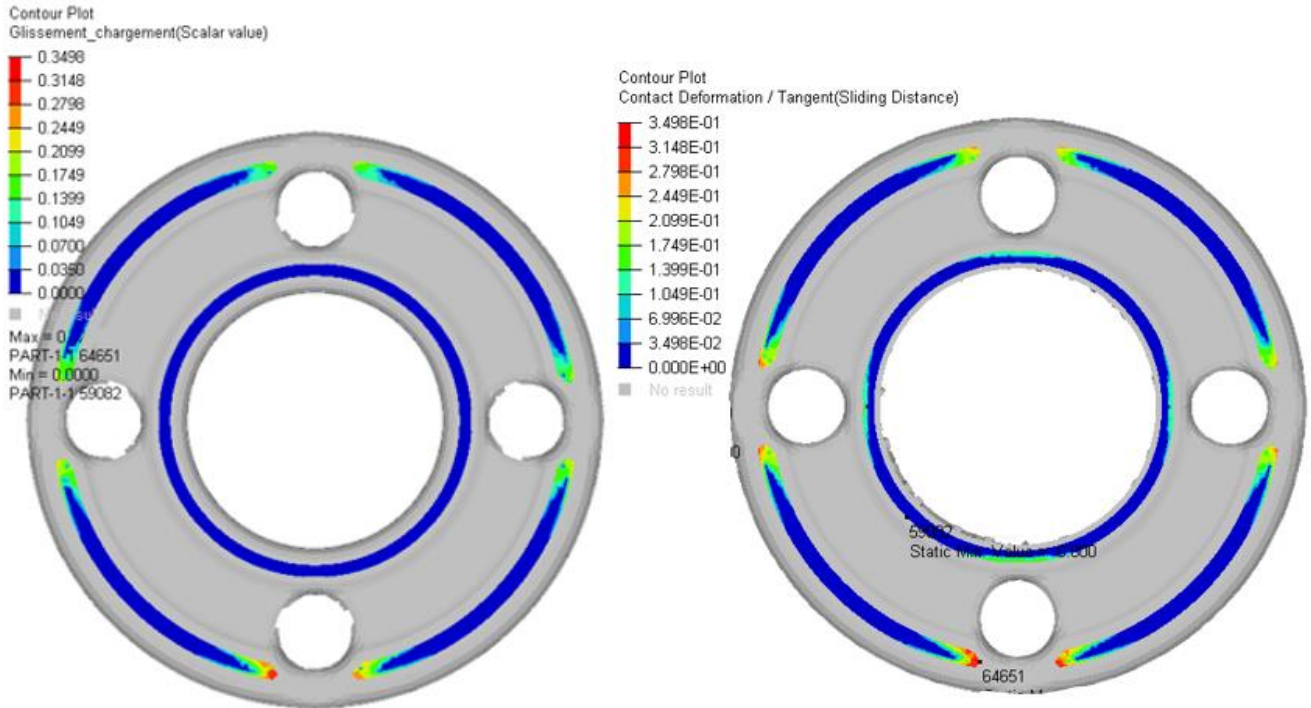


Figure 37 : Slip distances on the rim with the disk, with Abaqus (left) and OptiStruct (right)

Now concerning the slip between the disk and the hub, we notice more important differences between the models.

First of all, the slip distance is defined for locations where forces allow relative displacement of the parts in contact depending on the Coulomb contact definition. These locations are different between the Abaqus and OptiStruct models because of the meshes of the disk and the hub which are coarser. Moreover, the Surface to Surface contact characterisation defined at the hub and disk interface changed some of the contact location and the contact status of these parts together.

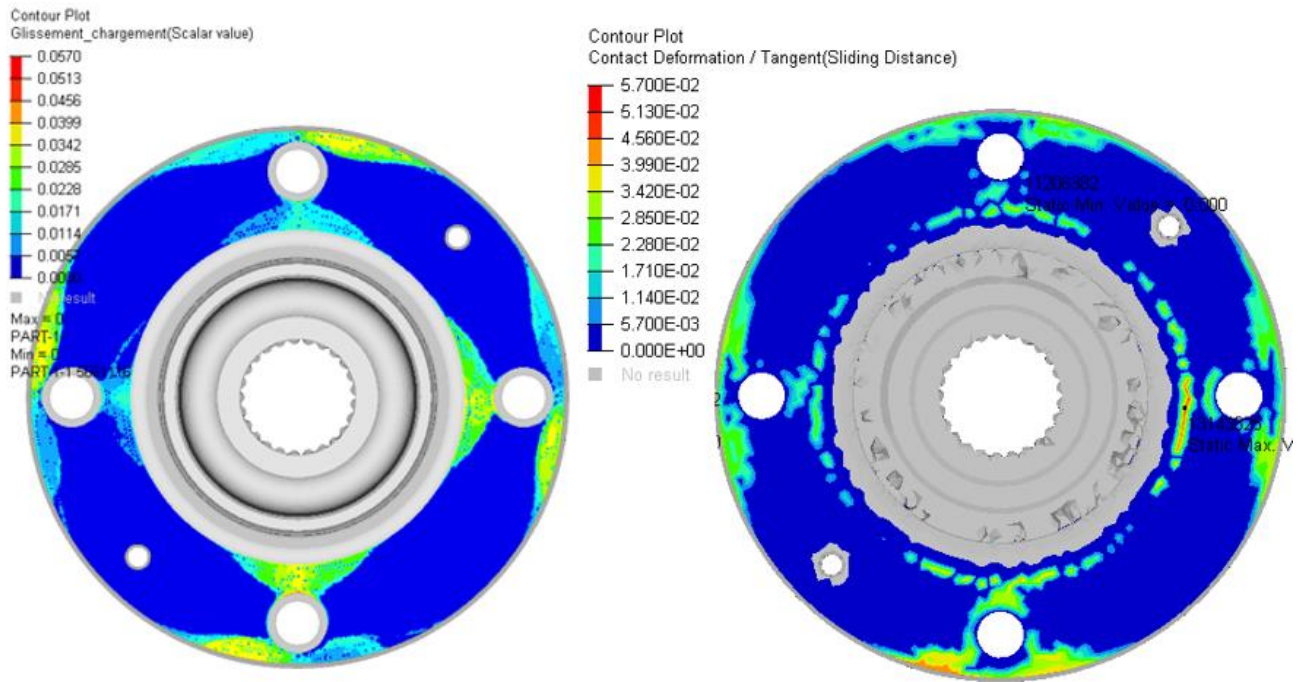


Figure 38 : Slip distances on the disk with the hub, with Abaqus (left) and OptiStruct (right)

4.8.3. Pressures comparison

We will now compare the different pressure values between the models, looking at both sides of the disk.

Concerning the side of the disk in contact with the hub, the pressures are quite different.

First of all, the values differ a lot and exceed 400MPa on various locations of the OptiStruct model when most locations of this side of the disk are below 300MPa in the Abaqus model. However, the OptiStruct model is more representative of reality as explained in part 4.4.1 thanks to the Surface to Surface contact definition, compared to the Abaqus model that uses Nodes to Surface contact. Hence the pressure at the very edges of the disk is lower on the OptiStruct model, as it should be since there is no contact there.

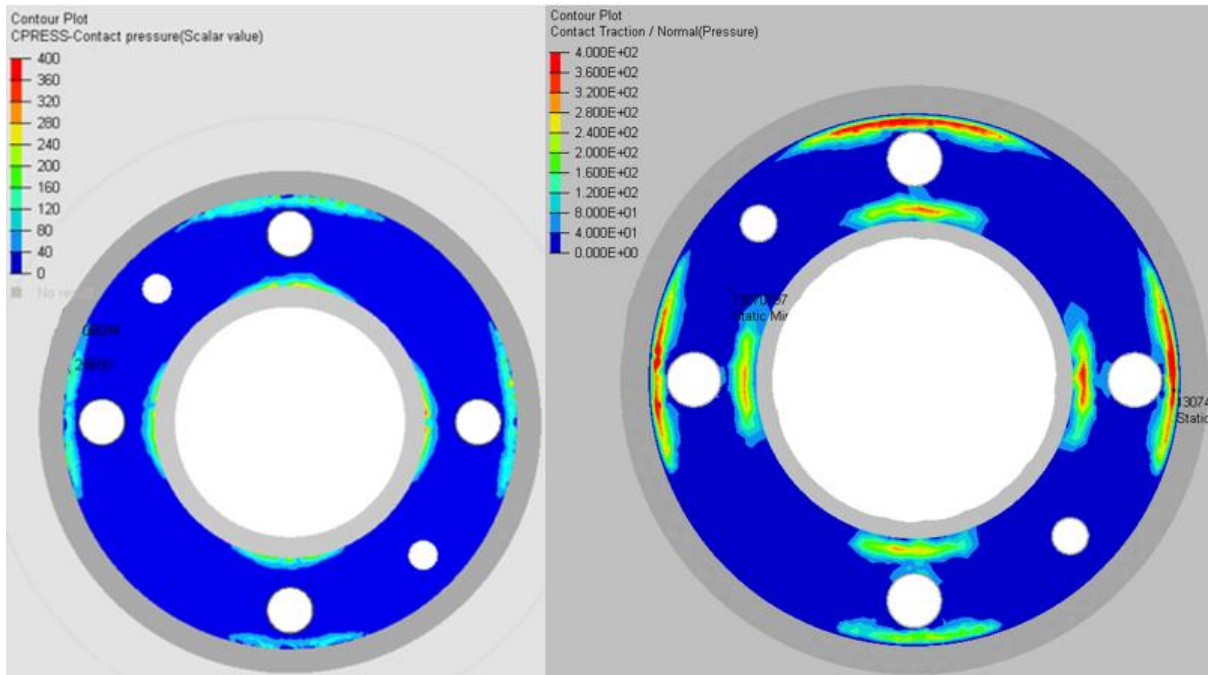


Figure 39 : Contact pressures between the disk and the hub, with Abaqus (left) and OptiStruct (right)

When it comes to the side of the disk in contact with the rim, the initial Surface to Surface contact characterisation was not an issue when post-processing this part of the model, so both Abaqus and OptiStruct models have the same contact definition, the only difference being the elements of the disk on the second one. We can see here the pressure values are rather close, as well as the maximum value not displayed here. Therefore, the pressure values in this disk are fairly well represented after the conversion.

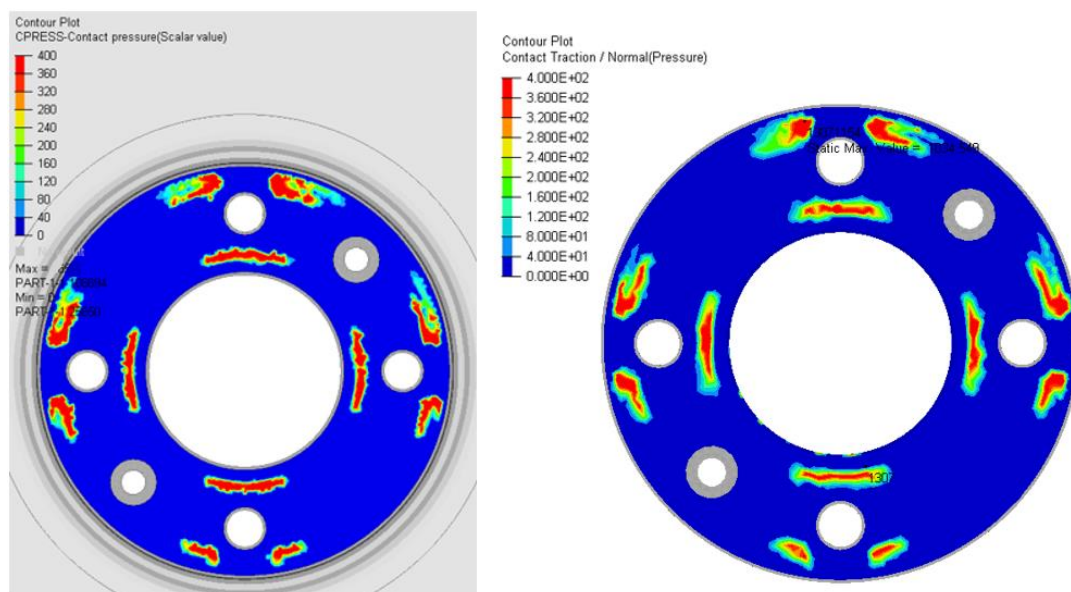


Figure 40 : Contact pressures between the disk and the rim, with Abaqus (left) and OptiStruct (right)

4.8.4. Screw angles and loosening

In order to better compare the results, it was also possible to compare the angle of the screws due to the load, as shown in the picture below. The angle is defined as \widehat{ABC} with A, B and C being on the neutral axis of the screw. A is at the bottom of the screw, B is at the same height as the hub (y-coordinate) and C is just before the pretension section where the tightening is applied.

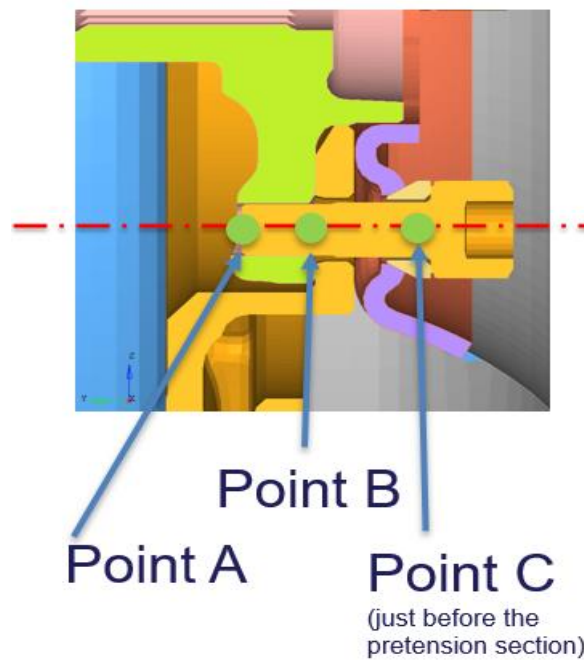


Figure 41 : \widehat{ABC} angle definition for post processing measurement

These measurements compared between the Abaqus and OptiStruct models show good similarities between them.

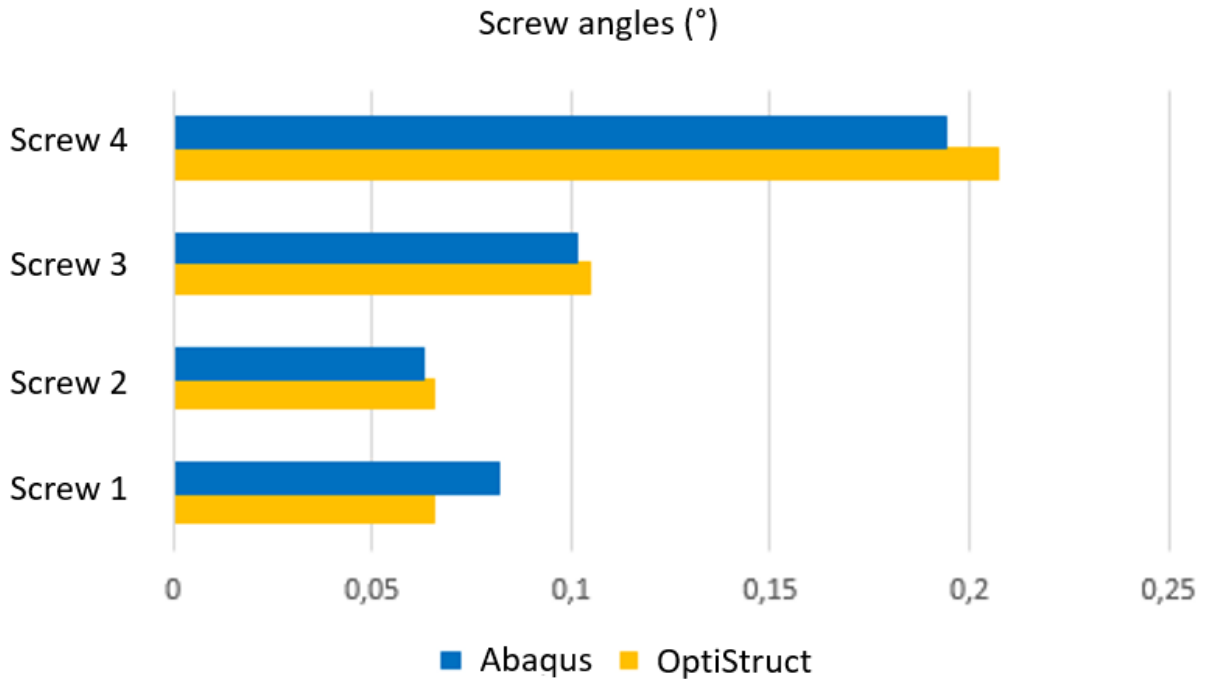


Figure 42 : Screw angles for the 2 models

It is normal the screw n°4 has a higher screw angle because it is the closest to the origin of the load. Despite a few differences, the bending seems to be correctly represented after the conversion.

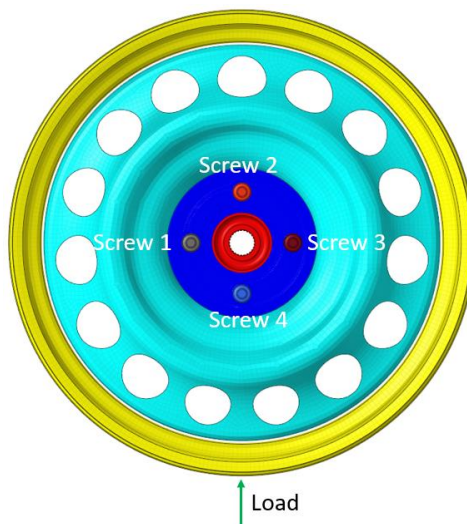


Figure 43 : Screws numbering on the wheel

Similarly, we can compare the tension in the screws due to the load applied to the wheel. This parameter is one of those we have to maximize in order to reduce self-loosening.

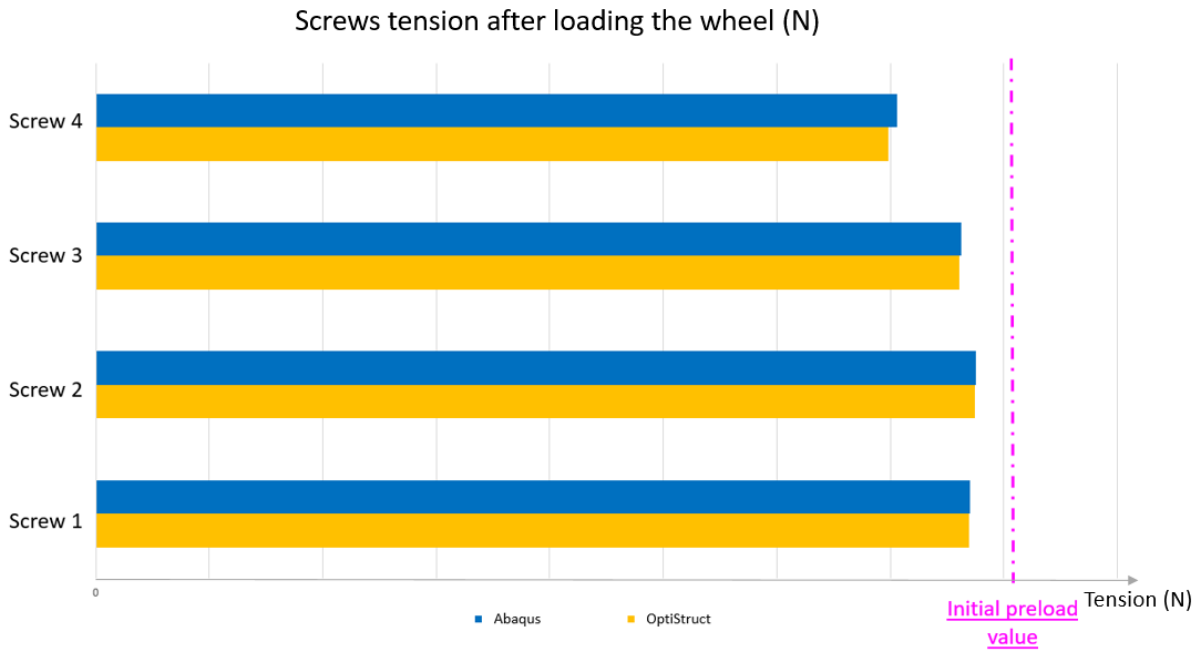


Figure 44 : Screws loads for the 2 models

The decrease in preload is extremely close, which shows how this parameter can confidently be optimized with this OptiStruct model.

4.9. Conversion conclusion

After converting the model from Abaqus to OptiStruct and comparing the different results, we concluded this new version was correct to be a good representation of the wheel. Indeed, the results of this OptiStruct model match those of the Abaqus one, except for those which did not fit reality, which actually got improved.

Therefore it is the model I will use and optimize in order to reduce loosening thanks to the previous study in part 3.

5. Wheel design optimization

5.1. Manual optimization

In order to optimize the design of the wheel, we will try to reduce the loosening of the screws. To do so, the parameter we will first study is the tension in the screws. Indeed the higher the tension in the screw after the load is applied to the wheel, the lower the loosening, as seen in the literature review. Hence, this screw tension is a good indicator. I will specifically look at the screw n°4 (at the bottom of the wheel, close to the load) since it is the one most likely to loosen according to the study made by Ksentini (8) and Manoharan (9).

The optimization will be conducted in 2 parts: firstly we try to get an idea of the behaviour of the tension relating to some parameters, secondly we use this relation to set the wheel with the optimal parameters which can maximise the final screws tension.

5.1.1. Linear and quadratic regressions

As a mean to approximate the curve of the screw tension depending on the different parameters, the method used here is a linear regression (and quadratic if necessary). By running multiple simulations while having different parameters vary, a linear regression should help get a linear function of the screw tension.

By noting \hat{y} the approximation of the tension based on n multiple parameters (x_1, \dots, x_n) , the screw tension y will be approximated as

$$y \approx \sum_{i=1}^{n+1} a_i x_i = \hat{y} \quad (5.1)$$

With $x_{n+1} \equiv 1$ so that a_{n+1} can represent the constant term in the linear expression.

The coefficients (a_1, \dots, a_{n+1}) are taken such that they minimize the error between y and \hat{y} with the 2-norm for the p tests taken into account.

Each of these tests gives 1 equation for 1 screw tension y_k and n+1 parameters, $x_{k,i}$ being the parameter x_i used in the k^{th} test. These p equations can be written as below:

$$y_k \approx \sum_{i=1}^{n+1} a_i x_{k,i} = \hat{y}_k \text{ with } k \in \llbracket 1, p \rrbracket$$

The proper way we chose to determine the coefficients (a_1, \dots, a_{n+1}) , was by minimizing the error between y and \hat{y} using the least squares model with the 2-norm:

$$\|e\|_2^2 = \|y - \hat{y}\|_2^2 = \sum_{i=1}^p (y_i - \hat{y}_i)^2 \quad (5.2)$$

In order to find the minimum of this $n+1$ -variable function, the gradient is determined for each coefficient:

$$\frac{\partial \|e\|_2^2}{\partial a_i} = -2 \sum_{k=1}^p (y_k - \hat{y}_k) x_{k,i} \quad \forall i \in \llbracket 1, n \rrbracket$$

Hence, we want to find the proper coefficients (a_1, \dots, a_{n+1}) which cancel this value for any i in $\llbracket 1, n \rrbracket$.

Using a matrix notation, we can have:

$$Y = \begin{pmatrix} y_1 \\ \vdots \\ y_p \end{pmatrix}, \hat{Y} = \begin{pmatrix} \hat{y}_1 \\ \vdots \\ \hat{y}_p \end{pmatrix}, A = \begin{pmatrix} a_1 \\ \vdots \\ a_{n+1} \end{pmatrix}, X = \begin{pmatrix} x_{1,1} & \cdots & x_{1,n+1} \\ \vdots & x_{i,j} & \vdots \\ x_{p,1} & \cdots & x_{p,n+1} \end{pmatrix}$$

Hence, the previous equation can transform to:

$$\frac{\partial \|e\|_2^2}{\partial a_i} = 0 \quad \forall i \in \llbracket 1, n \rrbracket \Leftrightarrow \sum_{k=1}^p (y_k - \hat{y}_k) x_{k,i} = 0 \quad \forall i \in \llbracket 1, n \rrbracket \quad (5.3)$$

$$\Leftrightarrow X^T(Y - \hat{Y}) = 0$$

$$\Leftrightarrow X^T(Y - XA) = 0$$

$$\Leftrightarrow A = (X^T X)^{-1} X^T Y \quad (5.4)$$

Since the matrix X has a full rank because we can choose its values, $\det(X^T X) \neq 0$ and $(X^T X)^{-1}$ exists.

In addition, $X^T X$ being a symmetric matrix, it is positive-definite, which means $A \mapsto \|Y - XA\|_2^2$ is convex and the solution for A ensuring the equation (5.3) is the only global minimum in \mathbb{R}^{n+1} .

This value given by equation (5.4) can ensure to approximate best most values of the screw tension without having to start more simulations.

Out of this approximation, we can gather interesting information:

- The Sum of Squares of residuals $SS_{res} = \sum_{i=1}^p e_i^2$ corresponds to how close the approximation is from the real values
- The coefficient of determination $R^2 = 1 - \frac{\sum_{i=1}^p e_i^2}{\sum_{i=1}^p (y_i - \bar{y})^2}$ corresponds to how representative the parameters (x_1, \dots, x_n) for the value y , with \bar{y} the average value of the y_k .

Hence, a R^2 close to 1 means the parameters we chose to minimize loosening (in our case by maximizing the screw tension) are enough, whereas a R^2 close to 0 means we lack many important parameters to characterize it.

This method is an overview of what Excel can do by itself with a series of data. However, we know not all processes can be explained properly with a linear expression which we can understand with the SS_{res} and R^2 parameters. Therefore, a quadratic regression can be used to better approximate the function of the screw tension with our parameters.

Since Excel can only do linear regressions for multiple parameters, it is possible to get quadratic regressions with no interaction between parameters by adding n other parameters (x_1^2, \dots, x_n^2) to the same linear regression method. Excel can thus solve this as a linear regression with $(x_1, \dots, x_n, x_1^2, \dots, x_n^2)$ parameters and $(a_1, \dots, a_n, a_{n+1}, \dots, a_{2n}, a_{2n+1})$ coefficients.

However, it needs about twice the experiments to accurately predict the value of the screw tension.

5.1.2. Optimization with parameters variations

A wheel model simulation takes on average about 2 hours to run using 32 processors. Thus it was possible to run up to 27 models with different parameter variations.

Moreover, since the coefficients of the matrix A are set to primarily fit the points given by the matrix X , we will add later some other values to check if the interpolation remains acceptable for these other points external to the approximation.

The parameters chosen to be optimized are the results of logical thinking and the study of Mehdi ZARWEL (7).

Indeed, he studies the impact of some parameters of a single-bolted assembly on loosening.

Among the parameters he explains have an impact on self-loosening, we will make vary the different friction coefficients in the model (only theoretically here since we cannot change the materials, but we hope some surface treatments could help us reach these optimal friction coefficients). Concerning the geometries, two parts of the rim are modelled using shell elements, making it easy to change their thickness. Similarly, we will change the arc of the inside of the rim as follows:

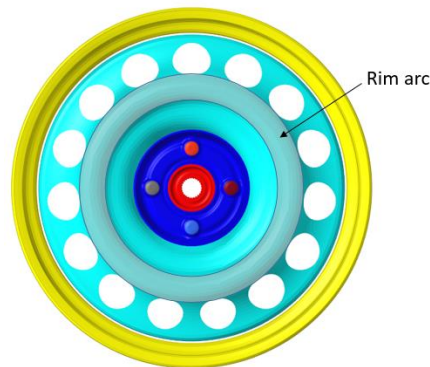


Figure 45 : Warped rim arc on the wheel

The arc of the warped rim can be represented as a conic between 3 points, with a specific ratio.

The initial rim arc with this representation had a ratio around 0.37 and a third point around $y=-52$.

The different variations of the rim design regarding these parameters had this ratio varying between 0.37 and 0.5, and the y coordinate of the third point between -70 and -80.

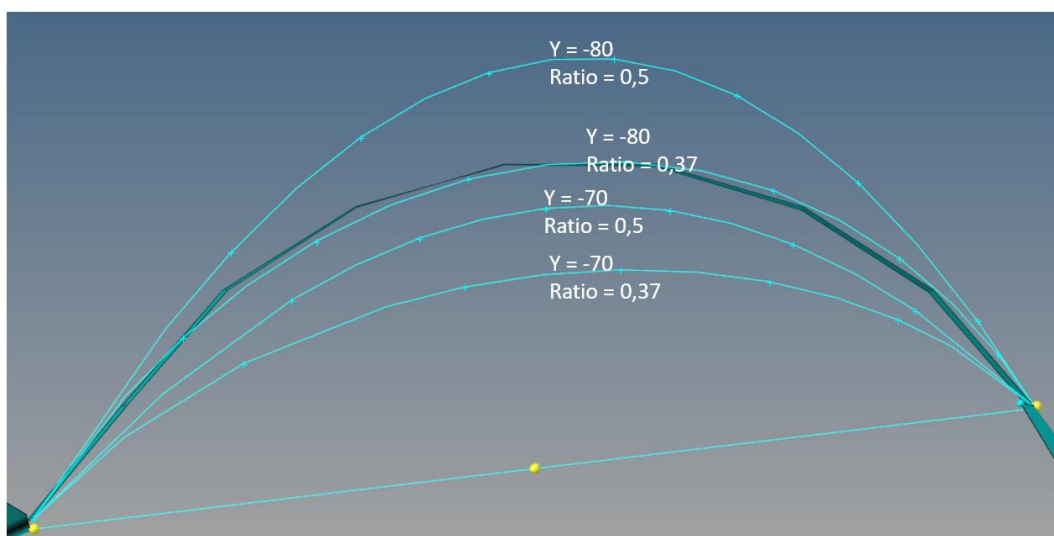


Figure 46 : Conics cross-section with third point y -coordinate and ratio

The different parameters can be summarized in the table below:

Parameter	Outer rim thickness	Inner rim thickness	Rim-Disk friction	Rim-Screw friction	Rim-Hub friction	Hub-Disk friction	Y coordinate	Ratio
Range	[2 ; 6]	[0,5 ; 3]	[0,07 ; 0,11]	[0,07 ; 0,11]	[0,07 ; 0,11]	[0,08 ; 0,12]	[-80 ; -70]	[0,37 ; 0,5]

Figure 47 : Parameters used for the manual optimization

Thanks to the 27 models run with different parameters, it was possible to extract a linear regression and a quadratic regression without interaction.

I ran 5 more models with different parameters from the ones used in the previous interpolation. The average error for the linear model is 0,187% and 0,063% for the quadratic interpolation. Moreover, the coefficient of determination R^2 for the linear model was 0.958 and it reached 0.995 for the quadratic model.

However, some coefficients for the quadratic regression reached around 75 000 which seemed quite high for such an approximation. Since I did not consider it necessary to use any lasso (least absolute shrinkage and selection operator) method, I preferred to keep the linear regression which had coefficients more than 10 times lower than the quadratic regression ones. Therefore I kept the linear regression to optimize these parameters for the self-loosening.

Using this approximation, the final expression of the screw tension can use the following coefficients:

Parameter	Constant	Outer rim	Inner rim	Rim-Disk friction	Rim-Screw friction	Rim-Hub friction	Hub-Disk friction	Y coordinate	Ratio
Coefficient	71074	183	21	-771	1616	421	4064	28	-480

Figure 48 : Coefficients of the linear regression

In order to choose the parameters which could maximize the screw tension, it is important to note that all parameters are taken without interaction in this formula. Moreover, each range is taken as a closed interval, therefore since this linear expression is continuous with respect to each parameter, the optimal value of a parameter can be given separately by maximizing its corresponding term with its coefficient, and the optimal value will either be the upper range or the lower range of the interval depending on the sign of the coefficient.

When computing the theoretical maximal screw tension value with these parameters, the linear regression gives an approximation at 70745N and we reach 70702N when it comes to the numerical simulation with these parameters. We can draw several conclusions from this.

Firstly, the theoretical screw tension given by the approximation gives of course the highest value among the ones previously run in the 32 tests, but the numerical value is also higher than any previously simulated value, which allows me to believe this approximation was decent, at least when accounting for these parameters.

Secondly, the error between this last approximation and the corresponding computed value is only 0,06%. This means although this optimal value was out of the range of the previous 27 tests, our approximation remains correct, which gives us even more confidence in the accuracy of our maximal value.

5.1.3. Shape changes

It is also possible to change the shape of some of the volumetric components to minimize loosening. However there is no precise trend on how to change this shape. The best rules to follow are to try to increase the overall stiffness of the parts as explained in equation (2.4).

Therefore the following improvements are not optimal but were tested after comparing the final screw tension in both cases.

I first changed the design of the rim in contact with the disk. I tried to increase the overall stiffness by filling in some holes of this side of the rim. After using Hypermesh to change the geometry, the final meshed design is as follows:

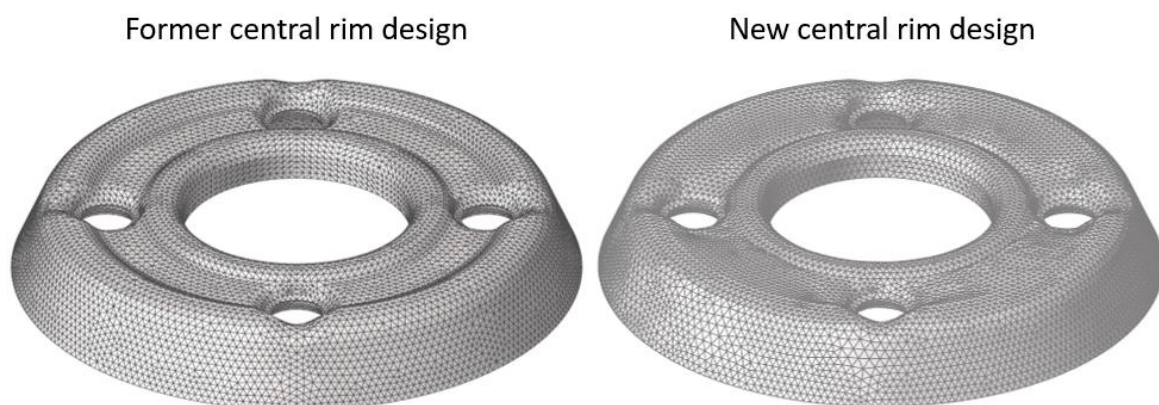


Figure 49 : Inner rim design improvement

Although the impact of the design on loosening also depends on other parameters, when using the parameters from the initial version (the 8 parameters listed for the linear regression in part 5.1.2) the screw tension loss decreased by 6% thanks to this new design only, and this decrease may slightly vary depending on the values of other parameters.

Similarly, I also changed the design of the cone of the screws, as well as its counterpart on the rim. I changed the angle of the cone from 60° to 39° to study the influence of this angle.

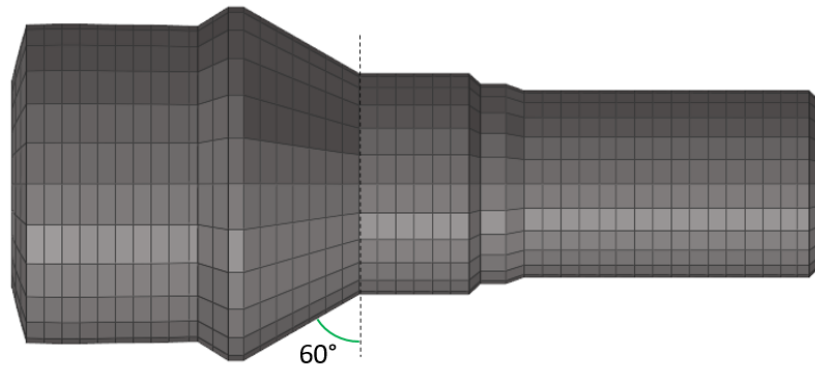


Figure 50 : Measurement of the angle of the cone on the screw

The final result on the rim part does not affect the previous improvement since the cones of the screws are on the other side. The final design of these screw holes is the following:

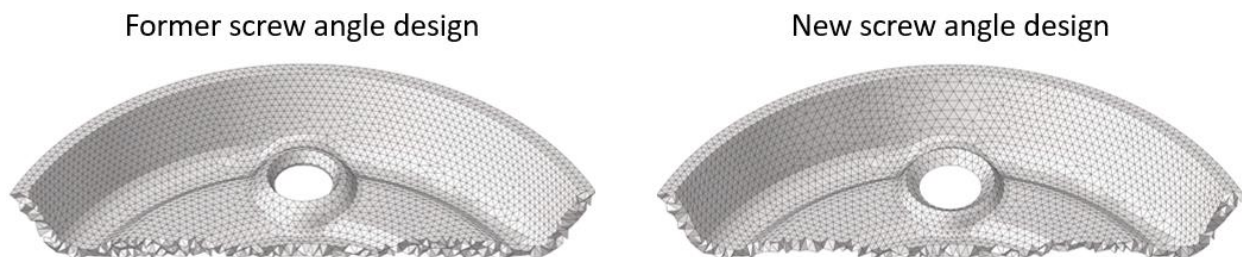


Figure 51 : Cones design improvement

I again ran a simulation with the same initial parameters as for the previous shape improvement. However the difference in screw tension was so low I concluded this angle had no real impact, but I should have tried more angles to carefully draw such a deduction if I had more time. Also the surface in contact between the screw and the rim was very similar in both designs, but increasing the contact surface between these parts would be very likely to reduce loosening. Hence I kept the initial cone version which did not require changing the cones.

Finally, the manually optimized wheel design considers the four friction coefficients and the two thicknesses, as well as the optimized warped rim arc and the new inner rim design.

The loss in screw tension for the 4th screw (dimensioning one) is lower than that of the initial wheel design by 21%.

5.2. Automatic optimization

OptiStruct software also enables the user to optimize a design automatically. It is therefore possible to minimize different parameters like the volume of the mass while keeping other parameters above or below a threshold value. Hence optimizing this wheel design using OptiStruct's automatic optimization tool could have been made by minimizing the loss in screw load (or possibly its lateral displacement considering Thomala's method) while keeping the shape inside a maximum volume envelope. However, my technical tutor and I faced numerous problems:

- OptiStruct optimization tool could not support non-linear large displacements analysis, so the only optimization possible would be with the hypothesis of small displacements, which could either give a good insight of the optimization, or complete non sense
- The current model contained 2 different loadsteps, i.e. the complete run of the model was made 1 step at a time, and it was not possible to specify the optimization to be made for the 2nd step only
- Finally the best parameter to optimize was the final screw tension, and the closest parameter we could find to optimize by the software was external forces, and not an internal force such as our screw load

In conclusion, I had to stick to the manual optimization to improve our model, although I know it might not be optimal, but the previous design improvements already led to some decent results.

5.3. Loosening prediction

In order to fully validate our optimized wheel model, we will now assess whether the screws can loosen due to the given load case. The loosening prediction will use Thomala's method confirmed by the localised slippage theory with equation (3.2).

The useful parameters of the screw are summarized below:

Parameter	Preload (N)	Friction coefficient (/)	Screw diameter (mm)	Useful screw length (mm)	Young's modulus (MPa)	Shear modulus (MPa)	Shear correction coefficient (/)	Critical displacement (mm)
Value	20 150	0,08	8	20	210 000	80 769	0,833	0,14

Figure 52 : Screw parameters to predict loosening of the wheel

The shear modulus was obtained with a Poisson's ratio of 0,3 and the second moment of area was computed with the diameter of the screw.

In comparison, we measure the actual displacement of the screw. It is important for the measurement to only consider the lateral displacement due to the loading, and no displacement caused by the first tightening step.

Therefore, the lateral displacement measured with HyperView is 0,075mm.

According to Thomala's method, the screw should not undergo spontaneous loosening with this load case.

6. Conclusion

The initial aim of this master thesis was to change the design of a given wheel model in order to minimize its loosening, and to better understand the spontaneous loosening process of screwed assemblies. The literature review has provided numerous examples and many details on the loosening aspects of a bolted assembly, as well as numerical, analytical and experimental studies on the subjects.

Firstly, it was necessary to properly define loosening; what I considered loosening, and how I could characterise and measure it. Indeed, loosening could be measured by the loss in screw preload as well as its rotation relative to the nut for a bolt, or to the upper part of the assembly for a screw. However, since loosening considers matting, strain hardening and even creep at the same time, it was more appropriate to measure it with screw tension loss rather than mere angle rotation to also take them into account. Therefore, the parameter to minimize in our case was the loss in screw tension after applying the load on the wheel.

Secondly, I developed Cobra and Thomala's methods to predict loosening on a general screwed assembly. The method with Cobra only considered analytical relations, with loosening occurrence depending on the external forces applied to the bolt compared to its preload. However, the various simulations ran with OptiStruct did not make any noticeable difference between the load cases where the assembly should witness spontaneous loosening and the others, thus the comparison with Cobra gave no usable result, since it was not possible to predict loosening with that method. When it comes to Thomala's method, this one compares the displacement of the screw head with the theoretical deflection of a beam with the same external forces. I used it on the previous assemblies, and the theoretical critical displacement was reached for a specific tangential load which corresponded to when half the screw head reached slipping with the upper plate. This half area of slip is also characterised as the transition between local slip and complete slip, which is the threshold value before reaching loosening, according to experimental and theoretical studies on local slippage. Hence this critical displacement corresponds to the start of loosening. I therefore considered Thomala's method accurate to determine loosening on this kind of screwed assembly.

Thirdly, since I know what to optimize, it is necessary to get a usable wheel model with OptiStruct, because the current model was only available with Abaqus. After completing the conversion, I followed with many comparisons with the post-treatment of the models to be sure both had very similar behaviours. Although it is hard to give a numerical value on the overall similarities between the models, the final results were close enough to consider the OptiStruct model properly converted.

Lastly, without considering Thomala's method first, minimizing loosening meant minimizing screw tension loss. Therefore the change in the wheel design had to minimize this parameter to reduce spontaneous loosening. I ran 27 wheel models with 8 different parameters in order to get an approximation of their influence on loosening. This provided me with a linear regression of the final screw tension, which led me to the optimal values of these 8

parameters. The overall friction between the parts has to be high, as well as the stiffness of the components, which meant a higher thickness for shell components. Finally, it is good to increase the stiffness of a component by changing its shape, but this is too shape-dependent to draw general conclusions on how to change the topology of the wheel to increase its stiffness, and numerical simulations can generally help by comparing shape designs one by one. I also manually changed other geometries of the design like the inner rim, since optimizing the topology automatically with OptiStruct was not possible. All of this taken into account, the optimal model I got for the wheel had a screw tension loss lowered by 21%. This optimized wheel model also seems to resist spontaneous loosening when applying Thomala's method.

7. Further possible research and improvements

The previous conclusion summarized the work done during the 5 months of my internship at Segula Technologies. I will explain here the possible work to further continue in order to go deeper into the design optimization of this wheel model.

Firstly, since this is an optimization, there is still room for improvement. When it comes to the design of the wheel and its shape, a lot of work could be done by a software like OptiStruct. Unfortunately, it was not possible during my internship, but it could potentially solve the whole topology optimization matter by itself if it was possible, although the limits of the shapes could be hard to set up.

Secondly, it can be interesting to accurately determine whether the screws will loosen due to the external load. The optimization has to minimize the loss in screw tension for the dimensioning screw. Therefore, this case has the lowest probability for any screw to loosen due to this load. It is also important to note that despite the wheel rotating along its axis when driving, this case where one screw is at the lowest point near the external force is where the screw is most likely to loosen, thus other cases will have better results. I unfortunately did not have time to improve a method similar to Thomala's but for screws with an angle for the cone and the upper plate, hence possible adjustments for this conical shape might be necessary to precisely assess on the possible loosening of a screw. Fortunately, these small adjustments could be neglected here since the critical displacement far exceeds the screw head deflection.

Lastly, predicting loosening by looking at the slip and stick regions only considers the area where slip could occur, which could be more representative of the phenomenon for some cases. In comparison, since a conical screw and a conical upper plate might get the screw head in contact with the upper plate before reaching the theoretical critical displacement, an equivalent of Thomala's method might not be accurate for any conical screw head because of this screw and plate penetration not being considered in the beams theories. Again, the screw deflection in our case is small enough to prevent any of this to happen.

When it comes to the optimized design of the wheel, this model is one of the theoretically best designs I could achieve with the different parameters I studied, but this still has to be proven experimentally. Moreover, every change in the model is not as easy to change in reality. Indeed, the friction coefficients could be changed to the optimal value without changing the materials by using surface treatments or other methods, but this is not sure and I did not study this part. Concerning all the shape designs, adding volume on the inner rim also adds weight which can be an issue. Concerning the shell parts and also this inner rim, their new designs might have them harder to produce, and some of the previous design changes were probably a compromise between non-loosening and several other characteristics I did not take into account like the ease of production, the weight or many others.

Sources

1. **Hao GONG, Jianhua LIU, Huihua FENG, Jiayu HUANG.** *Concept of radial slippage propagation triggering self-loosening and optimisation design of novel anti-loosening structures.* 2022.
2. **V. RAFIK, Bertrand COMBES, Alain DAIDIE, C. CHIROL.** *Experimental and Numerical Study of the Self-loosening of a Bolted Assembly.* 2019. hal-02119945.
3. **Hao GONG, Xiaoyu DING, Jianhua LIU, Huihua FENG.** *Review of research on loosening of threaded fasteners.* 2021.
4. **AZIZ, Hazem.** *Etude du dévissage spontané des assemblages boulonnés.* 2003.
5. **DELCHER, Christophe.** *Nouvelle approche pour la caractérisation du dévissage et desserrage des assemblages vissés.* *Matériaux & Techniques.* 2018.
6. **Bin Yang, Qingchao Sun, Qingyuan Lin, Lintao Wang, Xianlian Zhang, Yue Ma.** *Influence mechanism of bolted joint with geometric irregularity bearing surface on anti-loosening performance.* 2021.
7. **ZARWEL, Mehdi.** *Étude numérique et expérimentale du dévissage spontané des assemblages vissés.* 2016.
8. **KSENTINI, Olfa.** *Etude du dévissage spontané d'un assemblage boulonné soumis à des sollicitations transverses dynamiques.* 2016.
9. **Shiva Kumar Manoharan, Christoph Friedrich.** *Design and reliability on self-loosening of multi-bolted joints.* 2016.
10. **Yang, X & Nassar, S. A.** *Effect of Non-Parallel Wedged Surface Contact on Loosening Performance of Preloaded Bolts under Transverse Excitation.* 2011.
11. **Bin Yang, Qingchao Sun, Qingyuan Lin, Lintao Wang, Xianlian Zhang, Yue Ma.** *Influence mechanism of bolted joint with geometric irregularity bearing surface on anti-loosening performance.* 2021.
12. **Sawa, T., Ishimura, M. & Karami, A.** *A Bolt-Nut Loosening Mechanism in Bolted Connections under Repeated Transverse Loadings (Effect of inclined bearing surfaces on the loosening).* 2010.
13. **Rötscher, Felix.** *Die Maschinenelemente - Ein Lehr- und Handbuch für Studierende, Konstrukteure und Ingenieure.* 1927.
14. **VINCENT, Laurent.** *Maintenir le serrage des vis et des écrous. H7g6.* [En ligne] <https://www.h7g6.fr/data/article/34/maintenir-serrage-des-vis-des-ecrous>.